

12
BS

LEVEL II

NSWC TR 79-21

A073217

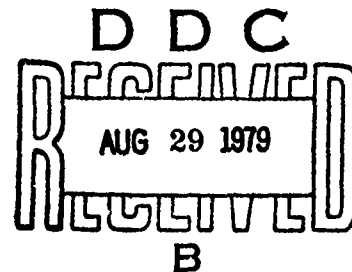
PREDICTIONS OF AERODYNAMIC HEATING ON TACTICAL MISSILE DOMES

BY T. F. ZIEN W. C. RAGSDALE

RESEARCH TECHNOLOGY DEPARTMENT

25 APRIL 1979

Approved for public release, distribution unlimited



DDC FILE COPY



NAVAL SURFACE WEAPONS CENTER

Dahlgren, Virginia 22448 • Silver Spring, Maryland 20910

79 08 28 032

UNCLASSIFIED

SECURITY CLASSIFICATION OF THIS PAGE (When Data Entered)

REPORT DOCUMENTATION PAGE		READ INSTRUCTIONS BEFORE COMPLETING FORM
1. REPORT NUMBER NSWC TR 79-21	2. GOVT ACCESSION NO.	3. RECIPIENT'S CATALOG NUMBER
4. TITLE (and Subtitle) PREDICTIONS OF AERODYNAMIC HEATING ON TACTICAL MISSILE DOMES		5. TYPE OF REPORT & PERIOD COVERED Technical report
7. AUTHOR(s) T. F. Zien and W. C. Ragsdale		6. PERFORMING ORG. REPORT NUMBER
9. PERFORMING ORGANIZATION NAME AND ADDRESS Naval Surface Weapons Center White Oak Silver Spring, Maryland 20910		8. CONTRACT OR GRANT NUMBER(s)
11. CONTROLLING OFFICE NAME AND ADDRESS 75 p		10. PROGRAM ELEMENT, PROJECT, TASK AREA & WORK UNIT NUMBERS 62332N; 00000; WF32396; 000000
14. MONITORING AGENCY NAME & ADDRESS (if different from Controlling Office) F32316, F32300		12. REPORT DATE 25 Apr 1979
		13. NUMBER OF PAGES 71
16. DISTRIBUTION STATEMENT (of this Report) Approved for public release, distribution unlimited		15. SECURITY CLASS. (of this report) Unclassified
17. DISTRIBUTION STATEMENT (of the abstract entered in Block 20, if different from Report) WF32396000, WF32300000		15a. DECLASSIFICATION/DOWNGRADING SCHEDULE
18. SUPPLEMENTARY NOTES		
19. KEY WORDS (Continue on reverse side if necessary and identify by block number) Aerodynamic Heating, Missile Domes, Boundary Layer Flows, Ablation, Transient Heat Conduction, Thermal Response of Missiles		
20. ABSTRACT (Continue on reverse side if necessary and identify by block number) The laminar heating on the hemisphere-cylinder configuration has been calculated using various predictive techniques in the Mach number range of one to five. The accuracy of these approximate results is assessed using the Cebeci-Smith finite difference code as a standard. A new procedure is suggested which is based on the consistent use of the Kays' semi-empirical formulas, and it appears to offer very accurate predictions of aerodynamic		

DD FORM 1 JAN 73 1473

EDITION OF 1 NOV 65 IS OBSOLETE
S/N 0102-014-6601

UNCLASSIFIED

SECURITY CLASSIFICATION OF THIS PAGE (When Data Entered)

391 596

UNCLASSIFIED

SECURITY CLASSIFICATION OF THIS PAGE(When Data Entered)

20. (continued)

heating on the configuration under study. A similar comparison on the turbulent heating predictions is also briefly discussed. In the transition region, a new approach of aerodynamic heating calculation based on the so-called "spot theory" is introduced, and some results are presented and discussed. Transient heat conduction inside the missile structure is studied using a new integral technique. ↗

UNCLASSIFIED

SECURITY CLASSIFICATION OF THIS PAGE(When Data Entered)

SUMMARY

The work reported herein was initiated in response to the interest and need expressed by the Aerothermodynamics personnel at the Naval Weapons Center, China Lake, California. This report contains the results obtained in the first phase of the project on aero-heating calculations where only the hemisphere-cylinder configuration was studied. Other configurations will be studied in the future.

This effort was supported by Naval Air Systems Command (NAVAIR) and executed for the Naval Weapons Center under the Strike Warfare Weaponry Technology Block Program under Work Request N00019-78-WR-81079, Airtask A03W-03P2/008B/7F32-3000-000 (appropriation 178 1319.1981). This airtask provides continued exploratory development in the air superiority and air-to-surface mission areas. Mr. W. C. Volz, AIR 320C, was the cognizant NAVAIR Technology Administrator.

Useful discussions with C. F. Markarian, W. R. Compton and B. Ryan in the course of this work are gratefully acknowledged.

Paul R. Wessel

PAUL R. WESSEL
By direction

ACCESSION for		
NTIS	Write Section	<input checked="" type="checkbox"/>
DDC	Buff Section	<input type="checkbox"/>
UNANNOUNCED		<input type="checkbox"/>
JUSTIFICATION _____		
BY _____		
DISTRIBUTION/AVAILABILITY CODES		
Dist.	Avail.	and/or SPECIAL
A		

CONTENTS

	<u>Page</u>
1. INTRODUCTION	7
2. AERODYNAMIC HEATING PREDICTION METHODS	8
2.1 Surface Pressure Distribution.	8
2.2 Aerodynamic Heating Calculations	10
2.2.1 Laminar Heating.	11
2.2.2 Turbulent Heating.	14
2.2.3 Transitional Heating	14
3. HEAT CONDUCTION CALCULATIONS	20
3.1 Basic Idea of the Integral Method--A Model Example	20
3.2 The Ablation Model	24
3.3 Power-Law Boundary Heat Flux - Present Method of Solution.	25
3.3.1 Preablation Solution	25
3.3.2 Ablation Solution.	27
4. CONCLUDING REMARKS	28
REFERENCES	29

ILLUSTRATIONS

<u>Figure</u>		<u>Page</u>
1	Missile Dome Configurations.	31
2a	Local Surface Pressure Coefficients on a Hemisphere.	32
2b	Local Surface Pressure Coefficients on a Hemisphere.	33
3	Local Surface Pressure Coefficients on a Hemisphere- Cylinder Downstream of the Shoulder.	34
4a	Velocity Distribution in a Hemisphere from Andrews' Eqn. for C_p	35
4b	Corrections to Velocity Distribution Computed from Andrews' Eqn.	35
5	Pressure Coefficients near the Stagnation Point on a Hemisphere from Andrews' Empirical Eqn.	36
6	Non-Dimensional Velocity Gradient at the Stagnation Point of a Hemisphere.	37
7	Configuration and Conditions used in Aeroheating Calculations	38
8a	Predicted Laminar Aerodynamic Heating on a Hemisphere- Cylinder	39
8b	Predicted Laminar Aerodynamic Heating on a Hemisphere- Cylinder	40
9	Predicted Turbulent Aerodynamic Heating on a Hemisphere- Cylinder	41
10a	Transitional Skin Friction for Incompressible Flat Plate Boundary Layer Flow, $Re_\theta = 200$	42
10b	Transitional Skin Friction for Incompressible Flat Plate Boundary Layer Flow, $Re_\theta = 400$	43
10c	Transitional Heating Predictions on a Hemisphere at $M = 5$	44
11a	Model Problem $\frac{d^2Y}{dX^2} = Y$; $Y(0) = 0$, $Y(1) = 1$	45
11b	Model Problem $\frac{d^2Y}{dX^2} = Y$; $Y(0) = 0$, $Y(1) = 1$	46
11c	Model Problem $\frac{d^2Y}{dX^2} = Y$; $Y(0) = 0$, $Y(1) = 1$	47
12	Ablation Model	48
13	Preablation Time for $q_0 = At^m$	49
14	Ablation Thickness, $q_0 = \text{const.}$	50

SYMBOLS

A	a constant
C_f	skin friction coefficient
C_p	pressure coefficient in eqn. (2.1)
C_p	heat capacity of air in eqns. (2.4), (2.6c), Btu/lbm $^{\circ}$ R
D	hemisphere diameter, ft
F	transitional skin friction and heating parameter (see pp.
f	temperature profile
G	spot formation rate parameter, 1/ft-sec
H	boundary layer shape factor
k	thermal conductivity
L_N	total length of nosetip, ft
M	Mach number
m	constant in eqn. (2.2); also exponent of the applied heat flux
P	local surface pressure, lbf/ft 2
P_r	Prandtl number
Q	local aerodynamic heating rate, Btu/ft 2 sec
Q_L	latent heat per unit mass
q_o	applied heat flux
R	hemisphere radius, ft
r	local body radius, ft
R_N	body radius at end of nosetip, ft
Re	Reynolds number
Re_x	length Reynolds number for flat plate boundary layer flow
Re_{θ}	Reynolds number based on boundary layer momentum thickness
S	distance along body surface measured from stagnation point, ft
St	Starton number
T	temperature, $^{\circ}$ R
t	time
U	velocity, ft/sec
X(t)	ablation front location
Δx	axial distance, measured from shoulder, ft
α	thermal diffusivity

β	velocity gradient at stagnation point (see p. 10), 1/sec; also, temperature profile parameter, eqn. (3.15)
γ	ratio of specific heats
$\overline{\gamma}$	intermittency factor in spot theory (see eqn. 2.13)
Δ	δ/δ_p
δ	temperature profile parameter
θ	local angle between dome surface normal and axis of symmetry in eqn. (2.1)
θ	boundary layer momentum thickness, ft; also, dimensionless temperature
μ	viscosity of air, lbm/ft-sec
ρ	density of air, lbm/ft ³
λ	dimensionless ablation thickness, eqn. (3.20)
ν	ablation parameter, $Q_L/C_p(T_p - T_\infty)$
ξ	dimensionless distance, eqn. (3.20)
τ	dimensionless time, eqn. (3.20)

Subscripts

aw	adiabatic wall
c	characteristic quantity
e	edge of boundary layer
n	normalized
p	phase-transition
w	wall
T	turbulent value
L	laminar value
∞	free stream; also condition at $x = \infty$ (conduction)
1	nondimensionalized with respect to characteristic quantity
90°	shoulder value

Superscripts

*	denotes value at start of transition
---	--------------------------------------

1. INTRODUCTION

Excessive thermal stress is known to be the main cause of mechanical failure of most long-range, high-speed missiles. Therefore, in the design of aerodynamic configurations for advanced tactical missiles, the ability to accurately predict the aerodynamic heating is essential.

The objective of this project is to develop efficient engineering procedures for predicting the aerodynamic heating on missile dome configurations related to the Navy's tactical missiles. The heating under consideration consists of convection from the boundary layer on the surface of the dome and conduction inside the structure; the two modes of heat transfer are coupled at the surface of the dome. In certain high speed missiles, plastic radomes are used which may be subject to ablation/charring during their long range flight. Therefore, the capability of treating conduction problems with phase transitions is also desirable.

In the present development of such engineering methods of aerodynamic heating calculations, the basic guidelines are simplicity and accuracy. The simplicity is dictated, to a large extent, by economic considerations because the method is to be used extensively for parametric studies. The starting point of the present work is the procedure of aerodynamic heating calculations currently used at the Naval Weapons Center¹ (NWC). The central part of this computation procedure is the finite difference code for two-dimensional conduction calculations, known as the SINDA code. The necessary boundary conditions for the conduction problem are provided by the empirical solution of the convective heating associated with the boundary layer flow over the dome configurations. However, the NWC procedure appears inadequate in certain applications, and the need for its improvement has become obvious.

In compliance with the aforementioned guidelines, the efforts in the present task are primarily directed towards developing, or improving, approximate (or empirical) techniques for aerodynamic heating calculations. We pursue the objective in two directions, one being to use the existing technology in the area and the other being to develop new technology to meet future needs.

In this report, some preliminary results of the effort are reported. Section 2 contains a description of a proposed scheme for laminar convective heating calculations and some comparisons with the scheme currently used by NWC. While the new scheme is based on existing formulas and is still empirical in nature, the accuracy seems significantly better than that of the current NWC scheme. An evaluation of the available methods for transitional and turbulent heating calculations is also included in this section. In section 3, a simple integral method for transient heat conduction calculations is presented along with its applications to a class of idealized ablation problems. This method is presented here as a potential candidate for use in the heat conduction

1. Compton, W. R., "Aerodynamic Heating of Spherically-Tipped Cylinders, Cones and Ogives, Using the General Thermal Analyzer SINDA," NWC TN 4061-172, Jun 1974.

calculations in the future. The results of this section represent the efforts in developing new technology for aerodynamic heating calculations. Finally, some concluding remarks and future plans are stated in section 4.

The three principal dome configurations used in tactical missiles are shown in Fig. 1. In this paper, results of convective heat transfer are presented only for the hemisphere-cylinder configuration. Application of the procedure to other configurations is not believed to cause basic difficulties as long as the surface pressure formulas can be satisfactorily verified, and results of the application will be reported in the future.

2. AERODYNAMIC HEATING PREDICTION METHODS

2.1 Surface Pressure Distribution

The starting point for predicting aerodynamic heating on a missile dome is the prediction of the surface pressure distribution on the dome, which is subsequently used to compute the local flow properties at the edge of the boundary layer. The dome geometries considered are all blunt bodies with detached shock waves at supersonic speeds, and local flow properties may be computed from a specified surface pressure distribution since the total pressure behind the normal shock wave at the stagnation point is related directly to the flight Mach number. In Ref. 2 an empirical equation developed by Andrews³ is shown to give accurate predictions of surface pressure on hemispheres and other bodies of revolution at Mach numbers above .75. This empirical equation is a modification of Newtonian flow theory, and has the following form:

$$C_p = C_{p_o} \cos^2 \theta + \frac{R_N}{L_N} \left\{ \frac{.78}{M_\infty^{2.27}} \sin \theta \cos \theta - \frac{.95 \sin \theta}{\exp[2.235(M_\infty - 1)]} \right\} \quad (2.1)$$

where

$$C_p = \text{local pressure coefficient} = \frac{2(p - p_\infty)}{\gamma M_\infty^2 p_\infty}$$

C_{p_o} = stagnation point pressure coefficient

L_N = total length of nosetip, ft

M_∞ = freestream Mach number

P = local surface pressure, lbf/ft²

P_∞ = freestream static pressure, lbf/ft²

R_N = body radius at end of nosetip, ft

γ = ratio of specific heats for air ($\gamma = 1.4$)

θ = local angle between dome surface normal and axis of symmetry.

2. Isaacson, L. K. and Jones, J. W., "Prediction Techniques for Pressure and Heat Transfer Distributions over Bodies of Revolution in High Subsonic to Low Supersonic Flight," NWC TP-4570, Nov 1968.
3. Andrews, J. S., "Steady State Airload Distribution on a Hammerhead Shaped Payload of a Multistage Vehicle at Transonic Speeds," Boeing Co. Rpt. D2-22947-1, Feb 1964.

The accuracy of equation (2.1) has been further tested in the present investigation by comparison with several additional sources of pressure data for the hemisphere-cylinder configuration^{4,5,6,7,8} including recent theoretical and experimental results from AEDC (Ref. 4). This comparison is shown in Figures 2a and 2b and it can be seen that the empirical equation compares favorably with the other sources of data. A simple exponential relationship was shown in Ref. 2 to give good results downstream of the shoulder. A comparison of predictions from this type of empirical relation with several sources of data is shown in Figure 3. The empirical equation used is as follows:

$$C_p = (C_p)_{90^\circ} \exp \left[- \frac{\Delta x / R_N}{2(m-.4)} \right] \quad (2.2)$$

where

$(C_p)_{90^\circ}$ = pressure coefficient at the shoulder (from Eq. (1))

$m = 1.2$, for $M_\infty < 1.2$

$= M_\infty$, for $M_\infty \geq 1.2$

Δx = axial distance, measured from shoulder

Note that C_p on the cylinder approaches zero as M_∞ increases.

The comparisons made indicate that equations (2.1) and (2.2) can be used to obtain reasonably accurate predictions of surface pressure on hemisphere-cylinders over the Mach number range of interest (1 to 5) in missile dome aerodynamic heating calculations. In using equation (2.1), however, it was found that a minor modification was necessary to obtain satisfactory results in the region near the stagnation point.

The local velocity at the edge of the boundary layer computed using equation (2.1) and one-dimensional flow relations⁹ was found to be linear with distance

4. Hsieh, T., "Flow-Field Study About a Hemisphere-Cylinder in the Transonic and Low Supersonic Mach Number Range," AEDC TR-75-114, Nov 1975.
5. Baer, A. L., "Pressure Distributions on a Hemisphere Cylinder at Supersonic and Hypersonic Mach Numbers," AEDE TN-61-96, Aug 1961.
6. Katz, J. R., "Pressure and Wave Drag Coefficients for Hemispheres, Hemisphere-Cones and Hemisphere-Ogives," NAVORD Rpt. 5849, Mar 1958.
7. Stine, H. A. and Wanloss, K., "Theoretical and Experimental Investigation of Aerodynamic-Heating and Isothermal Heat-Transfer Parameters on a Hemispherical Nose with Laminar Boundary Layer at Supersonic Mach Numbers," NACA-TN-3344, Dec 1954.
8. Morrison, A. M., et.al., "Handbook of Inviscid Sphere-Cone Flow Fields and Pressure Distributions - Volume I," NSWC/WOL/TR 75-45, Dec 1975.
9. Ames Research Staff, "Equations, Tables, and Charts for Compressible Flow," NACA Rpt. 1135, 1953.

along the surface (or angle θ) over most of the hemisphere, as shown in Figure 4a. This is in agreement with results from other investigations¹⁰. Close to the stagnation point however, the velocity is nonlinear and at Mach numbers above about 1.5 a value of zero velocity occurs at some distance from the stagnation point. This behavior is due to the fact that the empirical equation gives erroneous values of C_p close to the stagnation point, and values of C_p greater than $C_{p_{max}}$ occur at Mach numbers above 1.5, as shown in Figure 5. It should be noted that according to one-dimensional flow theory (Ref. 9):

$$\frac{dU_e}{d\theta} = - \frac{1}{\rho_e U_e} \frac{dp}{d\theta} \quad (2.3)$$

where

U_e = local velocity at edge of boundary layer, ft/sec

ρ_e = local density at edge of boundary layer, lbf-sec²/ft⁴

Since $U_e \rightarrow 0$ as $\theta \rightarrow 0$, $dU_e/d\theta$ can remain finite only if $dp/d\theta \rightarrow 0$ (and hence, $dC_p/d\theta \rightarrow 0$). This condition is satisfied by the pure Newtonian equation, but not by the empirical terms which have been added in equation (2.1). In the present investigation this difficulty was circumvented by projecting the lines of U_e/U_∞ versus θ to $\theta = 0$ and shifting each line by a constant value of $\Delta U_e/U_\infty$ so that $U_e/U_\infty = 0$ at $\theta = 0$. The correction factors used are shown in Figure 4b. Local pressures and pressure coefficients consistent with the adjusted values of local velocity were computed and used in the aerodynamic heating calculations. The adjusted values of C_p have been indicated in Figures 2 and 3 by dashed lines, and it can be seen that the changes in local C_p due to these adjustments were small.

The calculation of aerodynamic heating at the stagnation point requires that the velocity gradient at the stagnation point be known. Values of the non-dimensional velocity gradient $\beta D/U_\infty^*$ were evaluated from the curves of U_e/U_∞ versus θ shown in Figure 3 and have been compared with results from another investigation¹⁰ in Figure 6. The agreement is quite good.

2.2 Aerodynamic Heating Calculations

Aerodynamic heating rates calculated by the methods currently in use at the Naval Weapons Center (NWC)¹ have been compared with predictions from several other methods by the use of a specific example. The example chosen was that of a 3-inch diameter hemisphere-cylinder flying at Mach numbers ranging from 1 to 5 at an altitude of approximately 20,000 ft. The conditions for the calculations are listed in Figure 7.

10. Korobkin, I., "Laminar Heat Transfer Characteristics of a Hemisphere for the Mach Number Range 1.9 to 4.9," NAVORD Rpt. 3841, Oct 1954.

$$* \beta = \left(\frac{dU_e}{dS} \right)_0 = \frac{1}{R} \left(\frac{dU_e}{d\theta} \right)_0 = \frac{2}{D} \left(\frac{dU_e}{d\theta} \right)_0, \text{ 1/sec}$$

S = distance measured along surface, ft

2.2.1 Laminar Heating

The current prediction method¹ of NWC is first briefly described in the following. The method utilizes the stagnation point heating equation of Fay and Riddell²:

$$Q_o = .75 k_r^{-1/2} (c_p \mu_w)^{-1/4} (\rho_o \mu_o)^{-1/4} C_p (T_o - T_w) \sqrt{\left(\frac{dU_e}{ds}\right)_o} \quad (2.4)$$

where

Q_o = stagnation point heating rate, Btu/ft² sec

P_r = Prandtl number for air

ρ_o = air density evaluated at stagnation pressure and temperature, lbm/ft³

μ_o = viscosity of air evaluated at stagnation temperature, lbm/ft-sec

ρ_w = air density evaluated at stagnation pressure and wall temperature, lb/ft³

μ_w = viscosity of air evaluated at wall temperature, lbm/ft-sec

C_p = heat capacity of air at constant pressure = .24 Btu/lbm °R, assuming ideal gas properties

T_o = stagnation temperature, °R

T_w = wall temperature, °R

$\left(\frac{dU_e}{ds}\right)_o$ = stagnation point velocity gradient, 1/sec

Heating rates downstream of the stagnation point on the hemispherical dome are computed from the equation developed by Lees¹², based on a modified Newtonian pressure distribution:

$$\frac{Q}{Q_o} = \left\{ 2\theta \sin\theta \left[\left(1 - \frac{1}{\gamma M_\infty^2}\right) \cos^2\theta + \frac{1}{\gamma M_\infty^2} \right] \right\} / \sqrt{f(\theta)} \quad (2.5)$$

where

Q = local heating rate, Btu/ft²-sec

$$f(\theta) = \left[1 - \frac{1}{\gamma M_\infty^2} \right] \left[\theta^2 - \frac{\theta \sin 4\theta}{2} + \frac{1 - \cos 4\theta}{8} \right] + \frac{4}{\gamma M_\infty^2} \left[\theta^2 - \theta \sin 2\theta + \frac{1 - \cos 2\theta}{2} \right]$$

11. Fay, J. A. and Riddell, R. F., "Theory of Stagnation Point Heat Transfer to Dissociated Air," Journal of Aerospace Sciences, Vol. 25, No. 2, pp. 73-85, Feb 1958.
12. Lees, L., "Laminar Heat Transfer Over Blunt-Nose Bodies at Hypersonic Flight Speeds," Jet Propulsion, Vol. 26, No. 4, pp. 259-269, Apr 1956.

On the cylinder, the current method employs a semi-empirical relationship developed by Kays¹³ for aerodynamic heating on axisymmetric bodies. The following equation is based on the tabulated values given in Ref. 13 with the Prandtl number dependence incorporated for easy usage in later discussions

$$St = \frac{.33}{Pr^{2/3} \sqrt{R_{eL}}} \left(\frac{T_{aw}}{T_e} \right)^{-.12} \left(\frac{T_w}{T_{aw}} \right)^{-.08} \quad (2.6a)$$

where

$$St = \frac{Q}{\rho_e U_e C_p (T_{aw} - T_w)}$$

$$R_{eL} = \frac{\int_0^S r^2 (\rho_e U_e)^{1.87} dS}{\mu_e r^2 (\rho_e U_e)^{.87}} \quad (2.6b)$$

T_{aw} = the adiabatic wall temperature, °R

T_e = the local temperature at the edge of the boundary layer, °R

μ_e = the viscosity evaluated at the local edge temperature, lbm/ft-sec

r = the local body radius, ft

Heating rates computed from equations (2.5) and (2.6a) are matched at the hemisphere-cylinder junction and a constant pressure and local edge velocity are assumed on the cylinder.

Although equation (2.6a) is only utilized on the cylinder in the method currently used, its range of application includes axisymmetric bodies of general shape and according to Kays¹³ it may also be used at the stagnation point. At the stagnation point equation (2.6a) reduces to the following:

$$Q_o = .728 Pr^{-2/3} (T_w/T_o)^{-.08} (\rho_o \mu_o)^{.5} C_p (T_o - T_w) \sqrt{\left(\frac{dU_e}{dS} \right)_o} \quad (2.6c)$$

then, comparing equations (2.4) and (2.6c):

$$(Q_o)_{\text{Fay-Riddell}} \sim .76 Pr^{-.6} \left(\frac{\rho_w \mu_w}{\rho_o \mu_o} \right)^{.1}$$

13. Kays, W. M., Convective Heat and Mass Transfer, McGraw Hill, 1966

and,

$$(Q_o)_{\text{Kays}} \sim .728 \text{ Pr}^{-2/3} \left(\frac{T_w}{T_o} \right)^{-.08}$$

A comparison of Q_o values from equations (2.4) and (2.6c) over a range of possible flight conditions is given in the table below:

$$\text{Pr} = .7, T_\infty = -12^\circ\text{F}$$

M_∞	T_w/T_o	$\frac{(Q_o)_{\text{Kays}} - (Q_o)_{\text{Fay-Riddell}}}{(Q_o)_{\text{Fay-Riddell}}}$
1	.9	-1.2%
2	.6	-.4%
5	.35	+2.5%

In this comparison, the Sutherland viscosity law for air has been used to evaluate μ_w/μ_o . It can be seen that equations (2.4) and (2.6c) are in good agreement over this range of conditions.

Predictions of laminar aerodynamic heating by the method currently used have been compared with predictions obtained from a finite difference computer code¹⁴ and with predictions based on the consistent use of equation (2.6a) over the entire hemisphere-cylinder, utilizing local flow properties computed by the procedure outlined in section 2.1. The comparison of laminar heating predictions by these three methods is shown in Figures 8a and 8b. The results based on the consistent use of equation (2.6a) have been labeled "proposed procedure" in the figure. Comparisons are shown for Mach number 2 and above, since aerodynamic heating on missile domes is considered relatively unimportant below Mach 2. A slight inconsistency in this comparison should be mentioned. In the finite difference calculations a value of .72 was used for Pr, whereas a value of .7 was used in the current method and proposed method calculations. This inconsistency introduced roughly a 2 percent difference in the results, which is hard to detect on the scale to which the results have been plotted in Figure 8.

The finite difference method is considered to be accurate for laminar heating and is used here as a standard of comparison. It is seen that the predictions based on the presently proposed scheme are in good agreement with the finite difference method, particularly at the lower Mach numbers, and offer a significant improvement over the method currently used. Recent flight test data suggest that boundary layer transition may not occur on most IR domes at high altitudes, and consequently, the prediction of laminar heating rates should be of practical importance and interest.

14. Cebeci, T., Smith, A. M. O. and Wang, L. C., "A Finite-Difference Method for Calculating Compressible Laminar and Turbulent Boundary Layers," McDonnell Douglas Aircraft Co. Rpt. DAC-67131, Mar 1969.

2.2.2 Turbulent Heating

For turbulent heating, the method currently used employs a semi-empirical relationship developed by Kays¹³:

$$St = \frac{.0295}{Pr^{.4} (R_{e_T})^{.2}} \left(\frac{T_{aw}}{T_e} \right)^{-.6} \left(\frac{T_w}{T_{aw}} \right)^{-.4} \quad (2.7a)$$

where

$$R_{e_T} = \frac{\int_0^S (\rho_e U_e) r^{1.25} ds}{\mu_e r^{1.25}} \quad (2.7b)$$

Predictions by the current method have been compared with predictions obtained from the finite difference computer code¹⁴ and with predictions obtained from an equation developed by Vaglio-Laurin¹⁵ which is similar to that of Kays:

$$St' = \frac{.0296}{Pr^{2/3} (R'_{e_T})^{.2}} \left(\frac{\mu_e}{\mu_o} \right)^{.6} \quad (2.8a)$$

where

$$St' = \frac{Q}{\rho_e U_e C_p (T_o - T_w)}$$

$$R'_{e_T} = \frac{\int_0^S (\rho_e U_e) \mu_e r^{1.25} ds}{\mu_e^2 r^{1.25}} \quad (2.8b)$$

The comparison of turbulent heating predictions for Mach numbers 2 and 5 is shown in Figure 9. In this case the finite difference method cannot be used as a standard since empirical relations concerning turbulent transport must be utilized. The three methods compared appear to be in reasonably good agreement, especially near the shoulder of the hemisphere and on the cylinder. Further assessment of the turbulent prediction methods must involve comparisons with experimental data.

2.2.3 Transitional Heating

Downstream of the point where boundary layer transition begins skin friction and heat transfer rates increase rapidly from their laminar values to values

15. Vaglio-Laurin, R., "Turbulent Heat Transfer on Blunt-Nosed Bodies in Two-Dimensional and General Three-Dimensional Hypersonic Flow," Journal of Aerospace Sciences, Vol. 27, No. 1, Jan 1960.

approaching those for a completely turbulent boundary layer. The rapid increase of heating rates in the region of boundary layer transition is an important factor in determining thermal stresses in missile domes, making it desirable to predict heating in this region as accurately as possible. Several procedures exist for predicting transitional skin friction and/or heating rates, all of which are more or less empirical and are generally based on experimental data from flat plate experiments. In the following discussion, it is assumed that the location where transition starts, S^* , is given.

a. Persh/NWC Method

Persh¹⁶ developed a method for computing boundary layer growth in the transition region based upon the following equation for the skin friction:

$$C_f = C_{f_T} - \frac{\text{constant}}{Re_\theta^2} \quad (2.9)$$

The growth of the boundary layer in the transition region is computed using equation (2.9) and the boundary layer momentum equation:

$$\frac{d\theta}{dS} = \frac{C_f}{2} - \theta \left[(H+2) \frac{1}{U_e} \frac{dU_e}{dS} + \frac{1}{\rho_e} \frac{d\rho_e}{dS} + \frac{1}{r} \frac{dr}{dS} \right] \quad (2.10)$$

where

C_f = local skin friction coefficient

θ = boundary layer momentum thickness

Re_θ = Reynolds number based on momentum thickness

H = boundary layer shape parameter.

Subscript "T" denotes the fully turbulent value

The constant in equation (2.9) is determined by the condition $C_f = C_{f_L}$ at the start of transition, where C_{f_L} is the laminar value of the skin friction coefficient. Accordingly, equation (2.9) may be rewritten as follows:

16. Persh, J., "A Procedure for Calculating the Boundary-Layer Development in the Region of Transition from Laminar to Turbulent Flow," NAVORD Rpt. 4438, Mar 1957.

$$C_f = C_{f_T} - \left(\frac{Re_\theta^*}{Re_\theta} \right)^2 (C_{f_T}^* - C_{f_L}^*) \quad (2.11a)$$

or,

$$F = \left(\frac{Re_\theta^*}{Re_\theta} \right)^2 \left(\frac{C_{f_T}^* - C_{f_L}^*}{C_{f_T} - C_{f_L}} \right) \quad (2.11b)$$

where

$$F = \frac{C_{f_T} - C_f}{C_{f_T} - C_{f_L}}$$

Superscript * denotes values at the start of transition

Persh compared predictions from this procedure with experimental data for incompressible and compressible flow over flat plates and obtained reasonably good agreement in both cases. In order to apply the method to the more general case of boundary layer flow on axisymmetric bodies some method of evaluating the boundary-layer shape parameter, H is required. Persh developed a method for predicting H based on a correlation of velocity profile data for transitional boundary layers on flat plates. The involved nature of the required calculations makes the Persh method rather inconvenient to use except when combined with procedures which compute laminar and turbulent boundary layer growth by numerical integration of the integral boundary layer equations.

In using the Persh method for predicting transitional heating it is assumed that the parameter F has the same value for heating as for skin friction:

$$F = \frac{C_{f_T} - C_f}{C_{f_T} - C_{f_L}} = \frac{St_T - St}{St_T - St_L}$$

The current method used at NWC¹ to predict transitional heating rates is a modification of the Persh method, where the parameter F is related to the equivalent turbulent flat plate length Reynolds number as follows:

$$F = \left(\frac{Re_T^*}{Re_T} \right) \left(\frac{St_T^* - St_L^*}{St_T - St_L} \right) \quad (2.11c)$$

The integration used to obtain Re_T (equation 2.7b) is modified as follows:

$$Re_T = \frac{I^* + \int_{S^*}^S (\rho_e U_e) r^{1.25} dS}{\mu_e r^{1.25}} \quad (2.7c)$$

so that at S^* :

$$Re_T^* = \frac{I^*}{\mu_e^* r^{1.25}} \quad (2.7d)$$

The quantity I^* is determined by requiring Re_θ to be the same for the turbulent case as for the laminar case at S^* . In the NWC procedure:

$$\text{for the laminar boundary layer} \quad Re_\theta = .664 \sqrt{Re_L} \quad (2.12a)$$

$$\text{for the turbulent boundary layer} \quad Re_\theta = .037 (Re_T)^{4/5} \quad (2.12b)$$

combining the above gives:

$$Re_T^* = 36.9 (Re_L^*)^{5/8} \quad (2.12c)$$

and I^* follows from eq. (2.7d).

At S^* , the value of Re_T^* from equation (2.12c) is used in equation (2.7a) to compute St_T^* . At locations downstream of S^* values of St_T are computed from equations (2.7a) and (2.7c). Thus, the turbulent values of St used in the definition of F are based on an effective starting point for the turbulent boundary layer which is downstream of $S = 0$. In the Persh method an identical procedure is used to determine the turbulent values of the skin friction coefficient.

b. Spot Theory

Experimental investigations of transition on flat plates indicate that the transition region is characterized by the intermittent appearance of turbulent spots, which grow as they move downstream and finally merge to form the turbulent boundary layer. Emmons¹⁷ developed a theory for predicting skin friction in the transition region, based on the growth of turbulent spots, involving an intermittency factor defined as the fraction of time a given location is occupied by turbulent spots. All averaged properties such as skin friction and heating rate adjust smoothly from laminar to turbulent values as the intermittency factor increases from 0 to 1. Dhawan and Narasimha¹⁸ using flat plate data found that

17. Emmons, H. W., "The Laminar-Turbulent Transition in a Boundary Layer - Part I," Journal of Aerospace Sciences, Vol. 18, No. 7, pp. 490-498, Jul 1951.
18. Dhawan, S. and Narasimha, R., "Some Properties of Boundary Layer Flow During the Transition from Laminar to Turbulent Motion," Journal of Fluid Mechanics, Vol. 3, 1957-58.

the origin of turbulent spots takes place very nearly along a single line across the flow located at the beginning of transition. They found a universal intermittency distribution for flat plate flows and successfully predicted the skin friction and velocity profiles in the transition region. Chen and Tyson¹⁹ extended Emmons spot theory to include the case of boundary layers on blunt bodies. The parameter F is related to the intermittency factor, γ , from the turbulent spot theory as follows:

$$F = 1 - \bar{\gamma} \quad (2.13)$$

Chen and Tyson give the following relationships for $1 - \bar{\gamma}$, or F ¹⁹:

$$\text{for the flat plate:} \quad F = \exp \left[- \left(\frac{GS^{*2}}{U_e^*} \right) \left(\frac{S}{S^*} - 1 \right)^2 \right] \quad (2.14a)$$

$$\text{for a hemisphere:} \quad F = \exp \left[- \left(\frac{GS^{*2}}{U_e^*} \right) \ln \left(\frac{S}{S^*} \right) \ln \left(\frac{\tan \left(\frac{S}{2R} \right)}{\tan \left(\frac{S^*}{2R} \right)} \frac{\sin \left(\frac{S^*}{R} \right)}{\left(\frac{S^*}{R} \right)} \right) \right] \quad (2.14b)$$

where G = the spot formation rate parameter, 1/ft-sec
 R = hemisphere radius, ft

Chen and Tyson give the following relation for the dimensionless spot formation rate parameter:

$$\left(\frac{GS^{*2}}{U_e^*} \right) = \frac{(Re_S^*)^2}{R_{e\theta}^* 2.68 A^2} \quad (2.15a)$$

$$\text{where} \quad Re_S^* = \frac{\rho_e^* U_e^* S^*}{\mu_e^*}$$

$$A = 60 + 4.68 M_e^{*1.92} \quad (2.15b)$$

Equations (2.15a) and (2.15b) were obtained from a correlation of the extent of transition Reynolds number $Re_{\Delta S}$ as a function of the transition Reynolds number Re_S^* and edge Mach number, M_e , using data from flat plate experiments.

19. Chen, K. K. and Tyson, N. A., "Extension of Emmons' Spot Theory to Flows on Blunt Bodies," AIAA Journal, Vol. 9, No. 5, pp.821-825, May 1971.

c. Comparison

A comparison was made between values of the parameter F computed from the Persh method, the current NWC method and the Chen and Thyson method for the case of incompressible flow on a flat plate--this being the only case where results can be obtained in a straightforward manner from the Persh method. The definition of F in terms of the skin friction coefficient was used in the Persh and NWC methods and the following relations for incompressible flat plate boundary layer flow were utilized:

$$\text{laminar boundary layer: } \frac{C_f}{2} = \frac{.322}{\sqrt{Re_x}} = \frac{.220}{Re_\theta} \quad (2.16a)$$

$$\text{turbulent boundary layer: } \frac{C_f}{2} = \frac{.0296}{(Re_x)^{1/5}} = \frac{.013}{Re_\theta^{1/4}} \quad (2.16b)$$

where Re_x = the length Reynolds number for flat plate flow

The results of comparisons made for values of the momentum thickness Reynolds number at transition of 200 and 400 are shown in Figures 10a and 10b. In the figures, the parameter F has been plotted against the flat plate length Reynolds number measured from the beginning of transition, ΔRe_x .

Of the three methods compared, the Chen and Thyson method predicts the shortest extent of transition while the NWC method predicts the longest extent. The Persh method and Chen and Thyson method are in fairly good agreement over the initial part of the transition region at the transition Reynolds number of 400. Plotting ΔRe_x on a log scale as in Figures 10a and 10b makes it difficult to compare the gradients of skin friction predicted by the three methods. The NWC method predicts much higher gradients of skin friction (and/or heating) at the start of transition than the Chen and Thyson method, but lower gradients toward the end of transition. In the NWC method the steepest gradients occur near the start of transition whereas in the Chen and Thyson method they occur toward the middle of the transition region.

A final comparison of predictions for transitional heating is shown in Figure 10c. Here, predicted values of the parameter F are shown for the transitional boundary layer flow on a hemisphere at Mach 5. The conditions used in the boundary layer calculations are those shown in Figure 7 for a Mach number of 5, and transition was assumed to start 50 degrees from the stagnation point. Predictions by the Persh method have not been included due to the complexity of the calculations required for flow on a hemisphere. In Figure 10c predicted values of the parameter F from the NWC method and Chen and Thyson method have been plotted against the equivalent turbulent flat plate Reynolds number measured from the start of transition, ΔRe_T , obtained from equation (2.7c).

Predictions from the Chen and Thyson method using both the equation for a flat plate (2.14a) and the equation for a hemisphere (2.14b) are shown in Figure 10c. The difference between the two curves is very small indicating

there is little gained by using the more complicated function for the hemisphere. The comparison between the NWC and Chen and Thyson methods is essentially the same as the comparison for skin friction in incompressible flat plate flow.

In consideration of the comparisons made here it is felt that the method currently used at NWC probably overestimates the length of the transition region and does not give a good estimate of the gradient of heating in this region. Of the prediction methods considered, the method of Chen and Thyson was derived from more basic considerations than the other methods and rests upon a broader base of experimental data. It is felt that until more extensive comparisons are made with experimental data, this should be the preferred method for predicting transitional heating.

3. HEAT CONDUCTION CALCULATIONS

As stated in the Introduction, the present efforts also include the development of new technology for aerodynamic heating calculations. In this section a brief description of a new integral method will be presented. The method is currently under development into a practical tool for solving boundary layer flow and transient heat conduction problems alike.

The basic idea of the method will first be introduced by way of a simple example of an ordinary differential equation. The characteristic features of the method are explicitly demonstrated in the solution process of this model problem along with the principal merits of the method. A class of one-dimensional transient ablation problems is then solved by the present method as an example of application. Many details of the method are omitted from this paper to conserve space, but appear in Refs. (20, 21, 22).

3.1 Basic Idea of the Integral Method--A Model Example

The basic idea of the new integral method lies in the use of the integrated version of the governing differential equation as an expression for the boundary derivatives, after an approximate (guessed) solution is substituted for the unknown exact solution in the integrands. In physical applications, the boundary derivatives are often related to the important quantities of surface flux, e.g., skin friction (momentum flux), heating rates (heat flux), etc. on an aerodynamic vehicle. Their accurate and efficient predictions are of critical importance to the design and performance analysis of the vehicle.

20. Zien, T. F., "Approximate Calculation of Transient Heat Conduction," AIAA J., Vol. 14, No. 3, Mar 1976, pp. 404-406.
21. Zien, T. F., "Integral Solutions of Ablation Problems with Time-Dependent Heat Flux," AIAA Paper 78-864, 2nd AIAA/ASME Thermophysics and Heat Transfer Conference, Palo Alto, Calif., 24-26 May 1978. Also AIAA Journal, Vol. 16, No. 12, pp. 1287-1295, Dec 1978.
22. Zien, T. F., "A Simple Prediction Method for Viscous Drag and Heating Rates," Paper presented at the 1978 Science and Engineering Symposium (sponsored by USN/USAF), 17-19 Oct 1978, to appear in the Symposium Proceedings.

The basic idea will here be illustrated in terms of a simple boundary value problem of ordinary differential equation. While the model problem does not simulate exactly the mathematical structure of the physical problems intended for the application of the method, it does serve the purpose of exhibiting the general ideas in an elementary fashion for easy understanding.

Let us consider the following boundary value problem for the ordinary differential equation:

$$\frac{d^2 y}{dx^2} = y \quad 0 \leq x \leq 1 \quad (3.1)$$

$$y(0) = 0 \quad (3.2a)$$

$$y(1) = 1 \quad (3.2b)$$

The exact solution is easily obtained as

$$y = \frac{\sinh x}{\sinh 1} \quad (3.3a)$$

whereby the exact boundary derivatives are calculated as

$$\left(\frac{dy}{dx}\right)_0 = 0.8059; \left(\frac{dy}{dx}\right)_1 = 1.3130 \quad (3.3b)$$

These exact solutions will be used as a standard to determine the accuracy of the approximate integral solutions to be obtained.

One way to construct approximate solutions to the system, Eqs. (3.1) and (3.2), is to use polynomials which satisfy the boundary conditions, Eqs. (3.2a,b). Two such possible solutions are given below,

$$f_1 = Ax + (1 - A)x^2 \quad (3.4a)$$

$$f_2 = Ax^2 + (1 - A)x^3 \quad (3.4b)$$

where A is a constant referred to as the profile parameter. It is to be determined by requiring the approximate solutions to satisfy the integrated differential equation.

The integral of Eq. (3.1) has the form

$$\left(\frac{dy}{dx}\right)_1 - \left(\frac{dy}{dx}\right)_0 = \int_0^1 y dx \quad (3.5)$$

which will be used in the present method as the expression of the boundary derivatives when f is substituted for y in the integrand. In the elementary version of the present method, we assume that one boundary derivative, say, $(dy/dx)_1$ is determined by simply using

$$\left(\frac{dy}{dx}\right)_1 = \left(\frac{df}{dx}\right)_1 \quad (3.6)$$

Eq. (3.5) is then used in conjunction with an auxiliary equation for the determination of the two unknowns, $(dy/dx)_0$ and A . The auxiliary equation may be generated from a x-moment integral of Eq. (3.1) i.e.,

$$\int_0^1 x \frac{d^2 y}{dx^2} dx = \int_0^1 xy dx \quad (3.7)$$

Substitution of f for y in the integrands of Eq. (3.5) and Eq. (3.7) (using the boundary conditions, Eqs. (3.2), and assuming Eq. (3.6) leads to, respectively, the following equations:

$$\left(\frac{df}{dx}\right)_1 - \left(\frac{dy}{dx}\right)_0 = \int_0^1 f dx \quad (3.8)$$

and

$$\left(\frac{df}{dx}\right)_1 - 1 = \int_0^1 x f dx \quad (3.9)$$

Eqs. (3.8) and (3.9) then determine the quantities of A and $(dy/dx)_0$. The results are given below:

- (i) $f = f_1$: $A = 9/13$, $(dy/dx)_0 = 0.8589$ (+0.9%)
 $(dy/dx)_1 = (df_1/dx)_1 = 2 - A = 1.3077$ (-0.4%)
- (ii) $f = f_2$: $A = 12/7 = 1.7143$, $(dy/dx)_0 = 0.8929$ (+4.9%)
 $(dy/dx)_1 = (df_2/dx)_1 = 3 - A = 1.2857$ (-2.1%)

If in the solution process we choose to base the other boundary derivative on the approximate profile, i.e., $(dy/dx)_0 = (df/dx)_0$, then Eqs. (3.5) and (3.7) combine to determine A and $(dy/dx)_1$. The results are, for $f = f_1$,

$$A = 11/13 = 0.8462, (dy/dx)_1 = 7A/6 + 1/3 = 1.3205$$
 (+0.6%)
 $(dy/dx)_0 = (df_1/dx)_0 = A = 0.8462$ (-0.6%).

The percentage errors of these approximate values of the boundary derivatives are included in the parentheses. These approximate results are seen to be very accurate, even for the obviously erroneous profile of f_2 (zero profile slope at $x = 0$). Also, they exhibit rather mild dependence on the assumed approximate solution.

It is useful to compare these results with those of the classical integral method in order to demonstrate the inadequacy of the older method and the need for its improvement. This will now be carried out in the following.

In the classical method, the integrated differential equation, Eq. (3.5), is the only equation for the determination of the approximate profile, with both boundary derivatives taken directly from the approximate solution, i.e., $(dy/dx)_0 = (df/dx)_0$, $(dy/dx)_1 = (df/dx)_1$. The classical integral solutions are given below:

- (i) $f = f_1$: $A = 10/13 = 0.7692$, $(dy/dx)_0 = 0.7692$ (-9.6%)
 $(dy/dx)_1 = 1.2308$ (-6.3%)
- (ii) $f = f_2$: $A = 2.5385$, $(dy/dx)_0 = 0$ (-100%)
 $(dy/dx)_1 = 0.4615$ (-65%)

The above calculations clearly demonstrate the difficulties with the classical integral method. It is generally inaccurate, and very strongly depends on the (assumed) approximate profile. The latter difficulty makes the results unreliable, as there exists no unique way for choosing an approximate profile in the calculation of an actual physical problem. Note that the basic idea of the classical

method when applied to boundary-layer flow calculations leads to the well-known Karman-Pohlhausen's momentum integral technique.

In the present new integral method, the auxiliary equation can actually be generated in various different ways. One variant of the method is to use the y-moment integral of the basic differential equation.

In the y-moment scheme, the auxiliary equation takes the following form:

$$\left(\frac{dy}{dx}\right)_1 - \int_0^1 \left(\frac{df}{dx}\right)^2 dx = \int_0^1 f^2 dx \quad (3.10)$$

It will be assumed that $(dy/dx)_1 = (df/dx)_1$ in the following solution process.

Solution of Eqs. (3.8) and (3.10) gives the following results for $f = f_1$: (the other negative solution for A is discarded on physical grounds)

$$\begin{aligned} A &= 0.6826, \quad (dy/dx)_0 = 0.8703 \quad (+2.3\%) \\ (dy/dx)_1 &= (df_1/dx)_1 = 1.3174 \quad (+0.3\%) \end{aligned}$$

Again, the results are found to be very accurate, showing little variation from the previous results based on the x-moment scheme.

As a further illustration of the generalization of the new idea, we will exploit the combined use of the x-moment and the y-moment scheme in the approximate solution of the model problem. In this combined scheme, three equations are generated, i.e., Eqs. (3.5), (3.7) and (3.10), for the solution of three unknowns: A, $(dy/dx)_0$ and $(dy/dx)_1$.

For $f = f_1$, the results are

$$A = 0.7727, \quad (dy/dx)_0 = 0.8523 \quad (+0.2\%), \quad (dy/dx)_1 = 1.3144 \quad (+0.1\%)$$

which are practically indistinguishable from exact solutions.

The approximate solutions, f_1 and f_2 are plotted in Figs. 11a, b, c for both present method and the classical method. It is seen that the present solutions in the entire region $0 \leq x \leq 1$ do not show any substantial improvements over the classical ones, although the boundary derivatives calculated by the present method are far more accurate than those by the classical method. It is emphasized here again that in the present method, the boundary derivative is not taken from the boundary slope of the assumed profile.

This simple model problem serves to bring out the characteristic features of the new integral method. It is accurate and profile-insensitive, compared to the classical integral method. Its primary utility is the calculation of the boundary derivatives.

In the following, the application of the method to a class of idealized ablation problem will be presented as an example of the application of the method.

3.2 The Ablation Model

The model used here is a semi-infinite solid initially in a uniform temperature, T_∞ , lower than the phase-change temperature of the solid, T_p . An unsteady heat flux, $q_0(t)$, is then applied at the boundary until the boundary temperature reaches the phase-change temperature of the solid. This period is referred to as the preablation period. As the external heating continues, melting commences with the melting front progressing into the solid, and this period is referred to as the ablation period. In the idealized model, it is assumed that the molten solid is instantaneously and completely removed upon its formation say, by the action of some aerodynamic forces, so that the melting line acts like a new (moving) boundary upon which the external heat flux $q_0(t)$, acts. This assumption is particularly appropriate for the ablation of subliming materials such as comphor, graphite, etc. Also, to simplify the calculations, the thermophysical properties of the solid are assumed constant. This model is the same as the one used earlier by Landau²³, except that he considered only the special case of a constant q_0 , and obtained solutions by entirely numerical means. The model is sketched in Fig. 12.

In terms of this idealized model, the governing equations and boundary conditions are as follows:

(1) Preablation period.

$$\frac{\partial T}{\partial t} = \alpha \frac{\partial^2 T}{\partial x^2}, \quad t_p > t > 0, \quad \infty > x > 0 \quad (3.11)$$

$$T(x, 0) = T(\infty, t) = T_\infty \quad (3.12a)$$

$$-k \left(\frac{\partial T}{\partial x} \right)_{x=0} = q_0(t) \quad (3.12b)$$

where α and k are, respectively, the (constant) thermal diffusivity and heat conductivity of the solid. Also, t_p signifies the time at which the boundary temperature reaches T_p , i.e., $T(0, t_p) = T_p$.

(2) Ablation period.

$$\frac{\partial T}{\partial t} = \alpha \frac{\partial^2 T}{\partial x^2}, \quad \infty > t > t_p, \quad \infty > x > X(t) \quad (3.13)$$

$$T(x, t_p^+) = T(x, t_p^-) \quad (3.14a)$$

$$T(X, t) = T_p \quad (3.14b)$$

$$T(\infty, t) = T_\infty \quad (3.14c)$$

23. Landau, H. G., "Heat Conduction in a Melting Solid," Quarterly of Applied Mathematics, Vol. 8, 1950, pp. 81-94.

$$-k \left(\frac{\partial T}{\partial x} \right)_{x=X} + \rho Q_L \frac{dX}{dt} = q_o(t) \quad (3.14d)$$

Eq. (3.14a) ensures the continuity of the temperature distribution within the solid at the onset of ablation, $t = t_p$, and Eq. (3.14d) states the energy balance across the ablating front, $x = X(t)$. Note that the boundary condition, Eq. (3.14d), which relates the ablation speed, dX/dt , to the temperature gradient, $(\partial T/\partial x)_{x=X}$, is the basic source of the nonlinearity of the problem.

3.3 Power-Law Boundary Heat Flux - Present Method of Solution

The θ -moment scheme^{20,21} of the present integral method will be used in the calculations throughout this paper. Briefly speaking, the procedure makes a combined use of the heat balance integral (the integrated form of the heat equation) and the integral of the original heat equation after it is multiplied by $\theta (= T - T_\infty)$. A certain approximate temperature profile, f , is then substituted for the temperature in these integrated version of the heat equation. The heat balance integral based on the approximate temperature profile is used as the expression for the boundary heat flux.

3.3.1 Preablation Solution

Consider the idealized ablation problem with $q_o = At^m$, where A and m are constants. For the preablation period, an exponential profile for the temperature excess, $\theta = T - T_\infty$, is used in the calculation, i.e.,

$$f = \frac{q_o \delta}{k} \beta \exp \left(-\frac{x}{\delta} \right). \quad (3.15)$$

The profile contains two parameters, δ and β , and satisfies only the boundary of $\theta_\infty = 0$. Recall that the boundary flux is not to be obtained from $(\partial f/\partial x)_0$ in the present method^{20,21}. The preablation solutions have already been presented in Ref. (20), and will be briefly summarized here. The boundary temperature, T_o , in dimensionless form is given as

$$\theta_o \equiv \frac{k(T_o - T_\infty)}{q_o \sqrt{\alpha t}} = \sqrt{m+5/4} / (m+1) \quad (3.16)$$

The parameters δ and β are

$$\delta/\sqrt{\alpha t} = 2/\sqrt{4m+5} \quad (3.17a)$$

$$\beta = (m+5/4)/(m+1) \quad (3.17b)$$

As is shown in Ref. (20), the boundary temperature as given by Eq. (3.16) agrees better than 1% with the exact solution for all m in the range $0 \leq m < \infty$.

Ablation starts when $T_o = T_p$. From Eq. (3.16), the corresponding time, t_p , is determined as

$$t_p = \left[\frac{k(m+1)(T_p - T_\infty)}{A\sqrt{(m+5/4)\alpha}} \right]^{\frac{1}{m+1/2}} \quad (3.18a)$$

The "penetration depth", δ , at t_p follows from Eq. (3.17a),

$$\delta_p = \left[\frac{k(m+1)(T_p - T_\infty)\alpha^m}{A\sqrt{m+5/4}} \right]^{\frac{1}{2m+1}} / \sqrt{m+5/4}. \quad (3.18b)$$

The quantities t_p and δ_p are conveniently used as the scales for time and length, respectively, in the formulation of the ablation problem. However, since t_p and δ_p given above are only approximate solutions dependent on the method of solution, it appears desirable to use the characteristic time and length of the problem, t_c and ℓ_c , as the scales for easy determination of the absolute accuracy of the solutions. From a simple dimensional consideration, it is easily found that t_c and ℓ_c of the problem can be defined by

$$t_c = [k(\Delta T)/A\sqrt{\alpha}]^{1/(m+1/2)} \quad (3.19a)$$

and

$$\ell_c = \sqrt{\alpha t_c} = [k(\Delta T)\alpha^m/A]^{1/(2m+1)} \quad (3.19b)$$

where $\Delta T \equiv T_p - T_\infty$.

Thus, we introduce the following two sets of dimensionless variables in the ensuing calculations:

$$\xi \equiv \frac{x}{\delta_p}, \quad \tau \equiv \frac{t}{t_p}, \quad \Delta \equiv \frac{\delta}{\delta_p}, \quad \lambda \equiv \frac{X}{\delta_p} \quad (3.20a)$$

and

$$\xi_1 \equiv \frac{x}{\ell_c}, \quad \tau_1 \equiv \frac{t}{t_c}, \quad \Delta_1 \equiv \frac{\delta}{\ell_c}, \quad \lambda_1 \equiv \frac{X}{\ell_c} \quad (3.20b)$$

Note, in particular, that at the onset of ablation, $\tau_p = 1$ and

$$(\tau_{1p})_Z = [(m+1)^2/(m+5/4)]^{1/(2m+1)} \quad (3.21)$$

The accuracy of the present preablation solution may also be determined on the basis of a comparison of τ_{1p} as given by Eq. (3.21) with that given by the exact solution. The exact τ_{1p} can be found in Carslaw and Jaeger²⁴ as

24. Carslaw, H. S. and Jaeger, J. C., Conduction of Heat in Solids, 2nd ed., Oxford University Press, London, 1959, (Chap. 2).

$$(\tau_{1p})_E = [\Gamma(m + \frac{3}{2})/\Gamma(m+1)]^{1/(m + \frac{1}{2})} \quad (3.22)$$

where Γ is the Gamma function. It can be easily shown that τ_{1p} of the present solution approaches the exact limit of $\tau_{1p} = 1$ as $m \rightarrow \infty$.

The comparison between the approximate solution and the exact solution for τ_{1p} is shown in Fig. 13. The present solution is practically indistinguishable from the exact solution in the entire range of m , $\infty > m > 0$ in the figure, the maximum error being about 1.8% at $m = 0$. It is also interesting to note the existence of a maximum τ_{1p} near $m = 1.5$.

3.3.2 Ablation Solution

The ablation problem is then formulated in dimensionless form by using dimensionless variables $\xi, \tau, \Delta, \lambda$ and θ . The normalized temperature, $\theta = (T - T_\infty)/(T_p - T_\infty)$ is also used.

An exponential profile for θ is assumed,

$$f = \exp \left[- \frac{x - X(t)}{\delta(t)} \right] \quad (3.23)$$

where $X(t)$ is the (unknown) ablation line location, and $X(t_p) = 0$. Note that this choice of the temperature ensures the continuity of the temperature field at $t = t_p$ if $\delta(t)$ is assumed to be continuous at t_p .

With f substituting for θ , the following equations are easily derived from the ablation line condition, Eq. (3.14d), the integration of Eq. (3.13) from $\xi = \lambda$ to $\xi = \infty$, and the integration of the θ -moment of Eq. (3.13), respectively

$$-(m + 5/4) \frac{\partial \theta}{\partial \xi} \Big|_\lambda = (m + 1)\tau^m - \nu \frac{d\lambda}{d\tau} \quad (3.24a)$$

$$\frac{d\Delta}{d\tau} + \frac{d\lambda}{d\tau} = -(m + 5/4) \frac{\partial \theta}{\partial \xi} \Big|_\lambda \quad (3.24b)$$

$$\frac{1}{2} \frac{d\Delta}{d\tau} + \frac{d\lambda}{d\tau} = -(m + 5/4) \left[2 \frac{\partial \theta}{\partial \xi} \Big|_\lambda + \frac{1}{\Delta} \right] \quad (3.24c)$$

where $\nu = Q_L/C_p(T_p - T_\infty)$. Q_L is the latent heat of ablation per unit mass and C_p is the specific heat of the solid.

In the present procedure, Eqs. (3.24) form the system for the three unknowns, λ , Δ and the heat flux at the ablation front, $-(\partial \theta / \partial \xi)_\lambda$.

Closed-form solution can be obtained for the special case of $m=0$, i.e., the case of a constant heat flux. For other values of m , solutions are obtained easily by numerically integrating an ordinary differential equation (see Ref. (21)).

Typical results for $(m, \nu) = (0, \sqrt{\pi}/2)$ are shown in Fig. 14, compared with Landau's²³ numerical solution and the classical heat balance integral (HBI)

solution based on similar temperature profiles. Note that the ablation thickness in Fig. 14 is normalized by its value at $\tau = \infty$, i.e.,

$$\lambda_n \equiv \lambda/\lambda_\infty$$

where

$$\lambda_\infty = \tau^{m+1}/(1+\nu).$$

It is clear that the present solution is very accurate and shows considerable improvements over the HBI solution.

Admittedly, the example treated here is highly idealized. Nevertheless, the essential features of the mathematical system of ablation problems are included in the model. The success of the method in this application is therefore indicative of its potential for providing approximate solutions to realistic conduction problems in general and ablation problems in particular.

4. CONCLUDING REMARKS

In the present paper, an improved procedure for predicting laminar heating on the hemisphere-cylinder configuration is proposed. While the method is still empirical, it has been demonstrated to offer reliable solutions over a wide range of operating conditions and Mach numbers of interest to the Navy's tactical missiles. Inasmuch as the flight test data suggest laminar flow over most part of the missile dome, the improvement should be considered significant. For turbulent heating calculations, the current NWC scheme appears to be in reasonable agreement with the finite-difference calculations. However, since the exact solution to turbulent flow is not known at present, the agreement should not be viewed as a validation of the NWC scheme. The true confirmation could only come from a comparison with experimental data. In the transitional region, the method based on the idea of "spot formation" appears encouraging and warrants further study.

The transient conduction calculation presented in this paper is an example of the new technology being developed for future use in the aerodynamic heating studies. As the same basic ideas have been used in boundary layer calculations as well, the encouraging results presented here offer the hope of replacing the empirical schemes by this more rational approach in the future. A self-consistent procedure for aerodynamic heating calculations will then become available.

In the future, a similar study of the laminar heating will be conducted for the other principal dome configurations, such as the spherical ogive. The ultimate goal is to replace the empirical formulas currently in use by some more rational, yet still simple, predictive schemes.

The capabilities of calculating convective heating for three-dimensional configurations will also be developed in the course of the study.

REFERENCES

1. Compton, U. R., "Aerodynamic Heating of Spherically-Tipped Cylinders, Cones and Ogives, Using the General Thermal Analyzer SINDA," NWC TN 4061-172, Jun 1974.
2. Isaacson, L. K. and Jones, J. W., "Prediction Techniques for Pressure and Heat Transfer Distributions over Bodies of Revolution in High Subsonic to Low Supersonic Flight," NWC TP-4570, Nov 1968.
3. Andrews, J. S., "Steady State Airload Distribution on a Hammerhead Shaped Payload of a Multistage Vehicle at Transonic Speeds," Boeing Co. Rpt. D2-22947-1, Feb 1964.
4. Hsieh, T., "Flow-Field Study About a Hemisphere-Cylinder in the Transonic and Low Supersonic Mach Number Range," AEDC TR-75-114, Nov 1975.
5. Baer, A. L., "Pressure Distributions on a Hemisphere Cylinder at Supersonic and Hypersonic Mach Numbers," AEDE TN-61-96, Aug 1961.
6. Katz, J. R., "Pressure and Wave Drag Coefficients for Hemispheres, Hemisphere-Cones and Hemisphere-Ogives," NAVORD Rpt. 5849, Mar 1958.
7. Stine, H. A. and Wanloss, K., "Theoretical and Experimental Investigation of Aerodynamic-Heating and Isothermal Heat-Transfer Parameters on a Hemispherical Nose with Laminar Boundary Layer at Supersonic Mach Numbers," NACA-TN-3344, Dec 1954.
8. Morrison, A. M., et.al., "Handbook of Inviscid Sphere-Cone Flow Fields and Pressure Distributions - Volume I," NSWC/WOL TR 75-45, Dec 1975.
9. Ames Research Staff, "Equations, Tables, and Charts for Compressible Flow," NACA Rpt. 1135, 1953.
10. Korobkin, I., "Laminar Heat Transfer Characteristics of a Hemisphere for the Mach Number Range 1.9 to 4.9," NAVORD Rpt. 3841, Oct 1954.
11. Fay, J. A. and Riddell, R. F., "Theory of Stagnation Point Heat Transfer to Dissociated Air," Journal of Aerospace Sciences, Vol. 25, No. 2, pp. 73-85, Feb 1958.
12. Lees, L., "Laminar Heat Transfer Over Blunt-Nose Bodies at Hypersonic Flight Speeds," Jet Propulsion, Vol. 26, No. 4, pp. 259-269, Apr 1956.

13. Kays, W. M., Convective Heat and Mass Transfer, McGraw Hill, 1966 (Chap. 10, 11, 13)
14. Cebeci, T., Smith, A. M. O. and Wang, L. C., "A Finite-Difference Method for Calculating Compressible Laminar and Turbulent Boundary Layers," McDonnell Douglas Aircraft Co. Rpt. DAC-67131, Mar 1969.
15. Vaglio-Laurin, R., "Turbulent Heat Transfer on Blunt-Nosed Bodies in Two-Dimensional and General Three-Dimensional Hypersonic Flow," Journal of Aerospace Sciences, Vol. 27, No. 1, Jan 1960.
16. Persh, J., "A Procedure for Calculating the Boundary-Layer Development in the Region of Transition from Laminar to Turbulent Flow," NAVORD Rpt. 4438, Mar 1957.
17. Emmons, H. W., "The Laminar-Turbulent Transition in a Boundary Layer--Part I," Journal of Aerospace Sciences, Vol. 18, No. 7, pp. 490-498, Jul 1951.
18. Dhawan, S. and Narasimha, R., "Some Properties of Boundary Layer Flow During the Transition from Laminar to Turbulent Motion," Journal of Fluid Mechanics, Vol. 3, pp. 418-436, 1957-58.
19. Chen, K. K. and Thyson, N. A., "Extension of Emmons' Spot Theory to Flows on Blunt Bodies," AIAA Journal, Vol. 9, No. 5, pp. 821-825, May 1971.
20. Zien, T. F., "Approximate Calculation of Transient Heat Conduction," AIAA J., Vol. 14, No. 3, pp. 404-406, Mar 1976.
21. Zien, T. F., "Integral Solutions of Ablation Problems with Time-Dependent Heat Flux," AIAA Paper 78-864, 2nd AIAA/ASME Thermophysics and Heat Transfer Conference, Palo Alto, Calif., 24-26 May 1978. Also, AIAA Journal, Vol. 16, No. 12, pp. 1287-1295, Dec 1978.
22. Zien, T. F., "A Simple Prediction Method for Viscous Drag and Heating Rates," Paper presented at the 1978 Science and Engineering Symposium (sponsored by USN/USAF), 17-19 Oct 1978, to appear in the Symposium Proceedings.
23. Landau, H. G., "Heat Conduction in a Melting Solid," Quarterly of Applied Mathematics, Vol. 8, 1950, pp. 81-94.
24. Carslaw, H. S. and Jaeger, J. C., Conduction of Heat in Solids, 2nd ed., Oxford University Press, London, 1959, (Chap. 2).

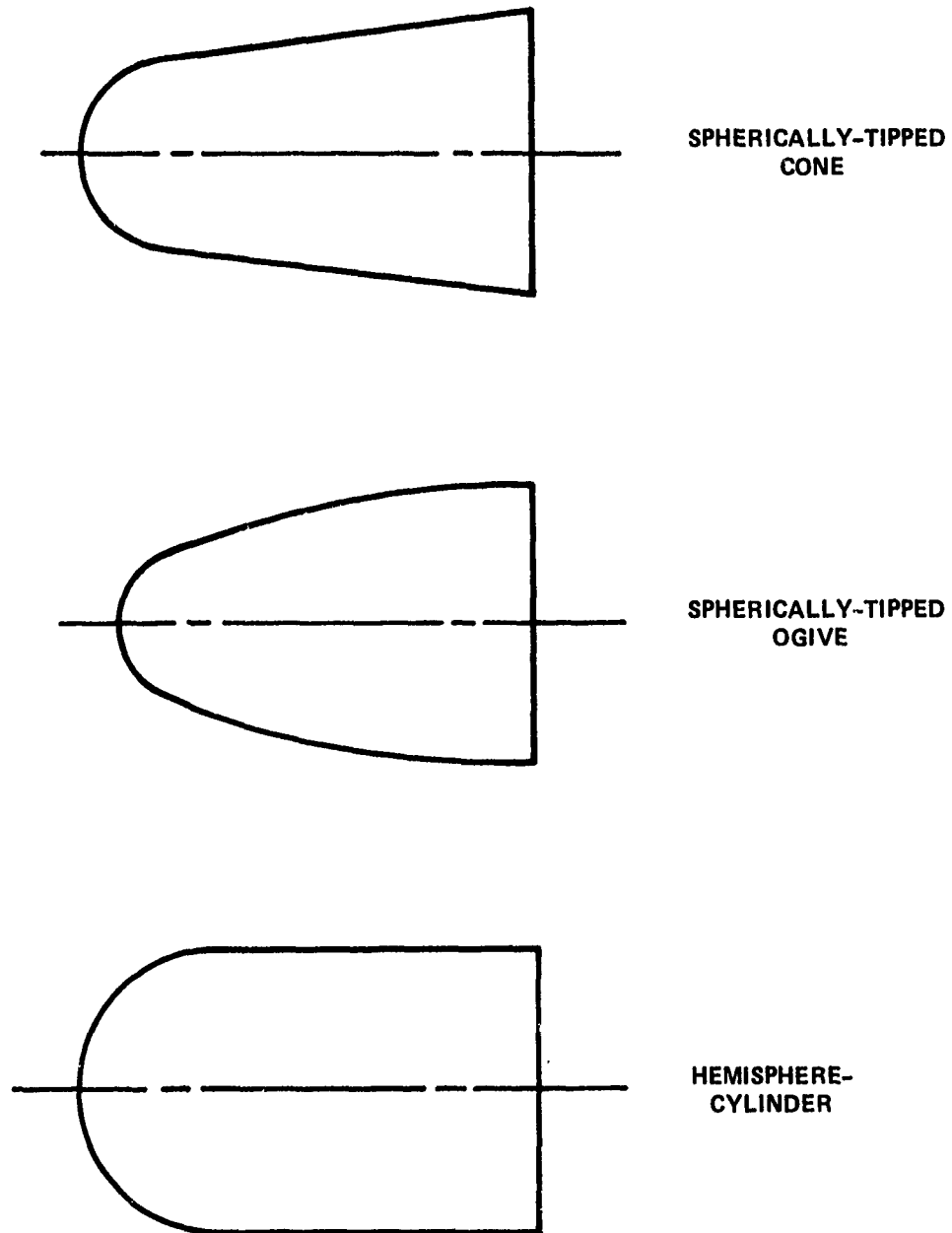


FIGURE 1. MISSILE DOME GEOMETRIES

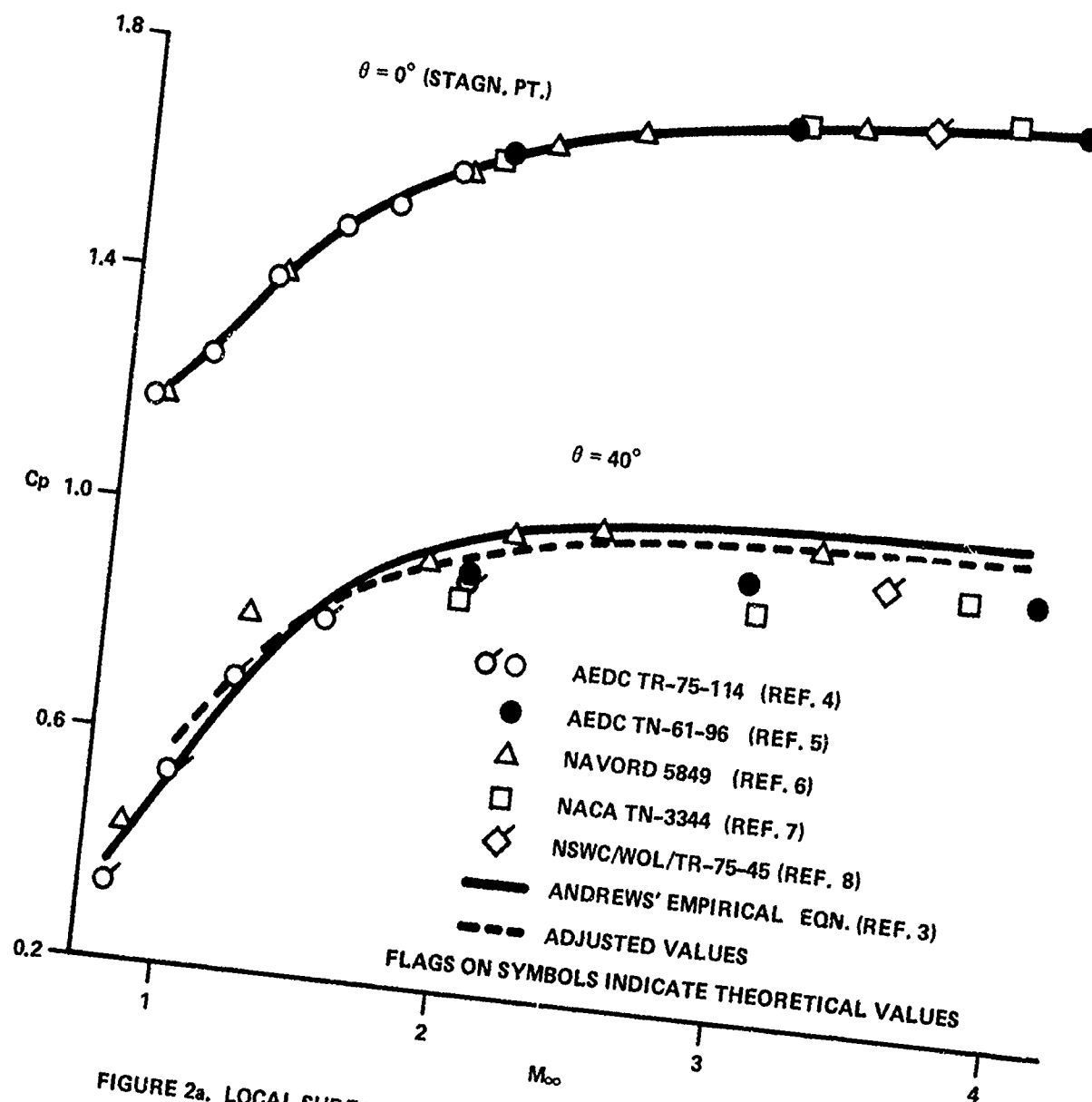


FIGURE 2a. LOCAL SURFACE PRESSURE COEFFICIENTS ON A HEMISPHERE

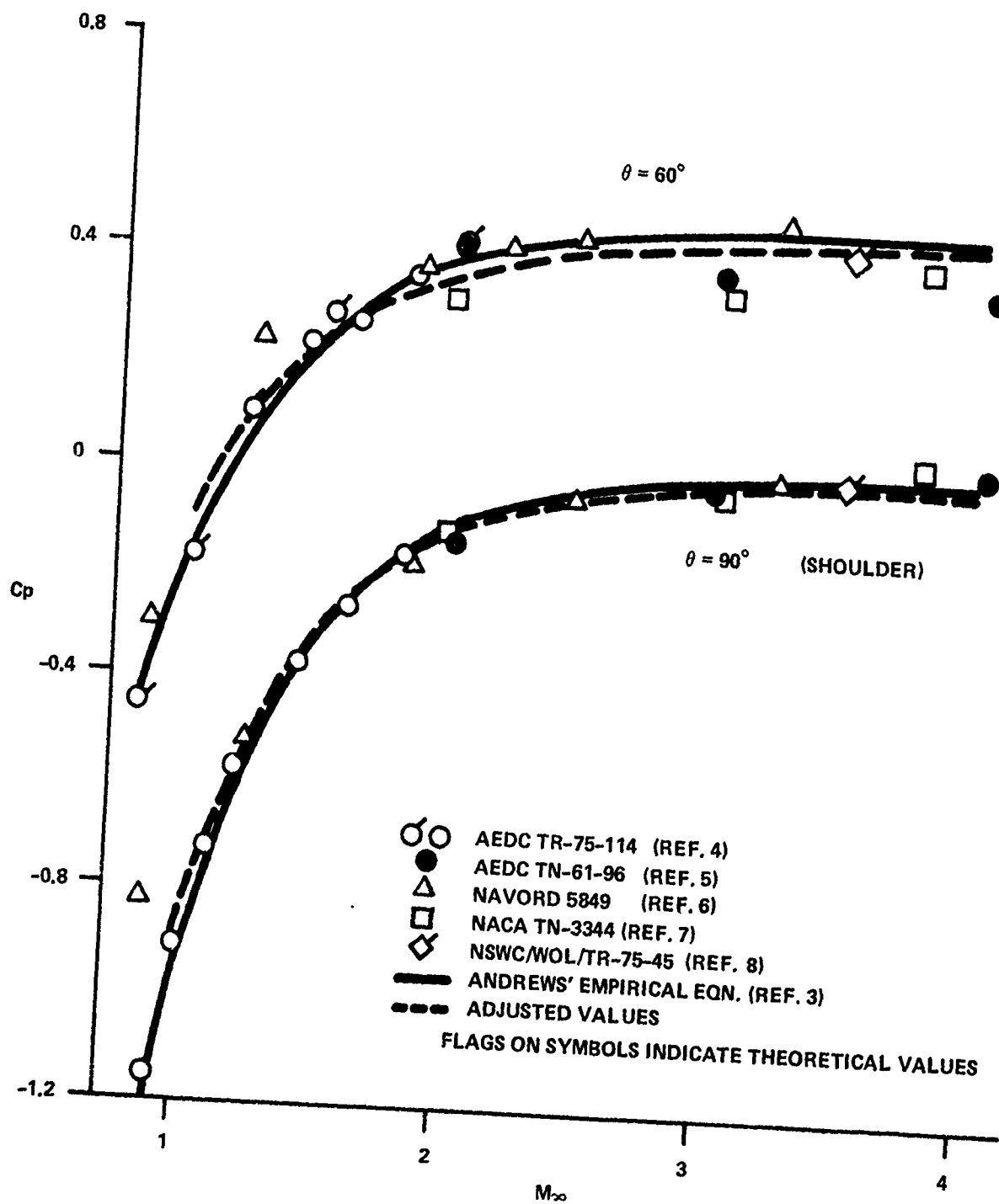


FIGURE 2b. LOCAL SURFACE PRESSURE COEFFICIENTS ON A HEMISPHERE

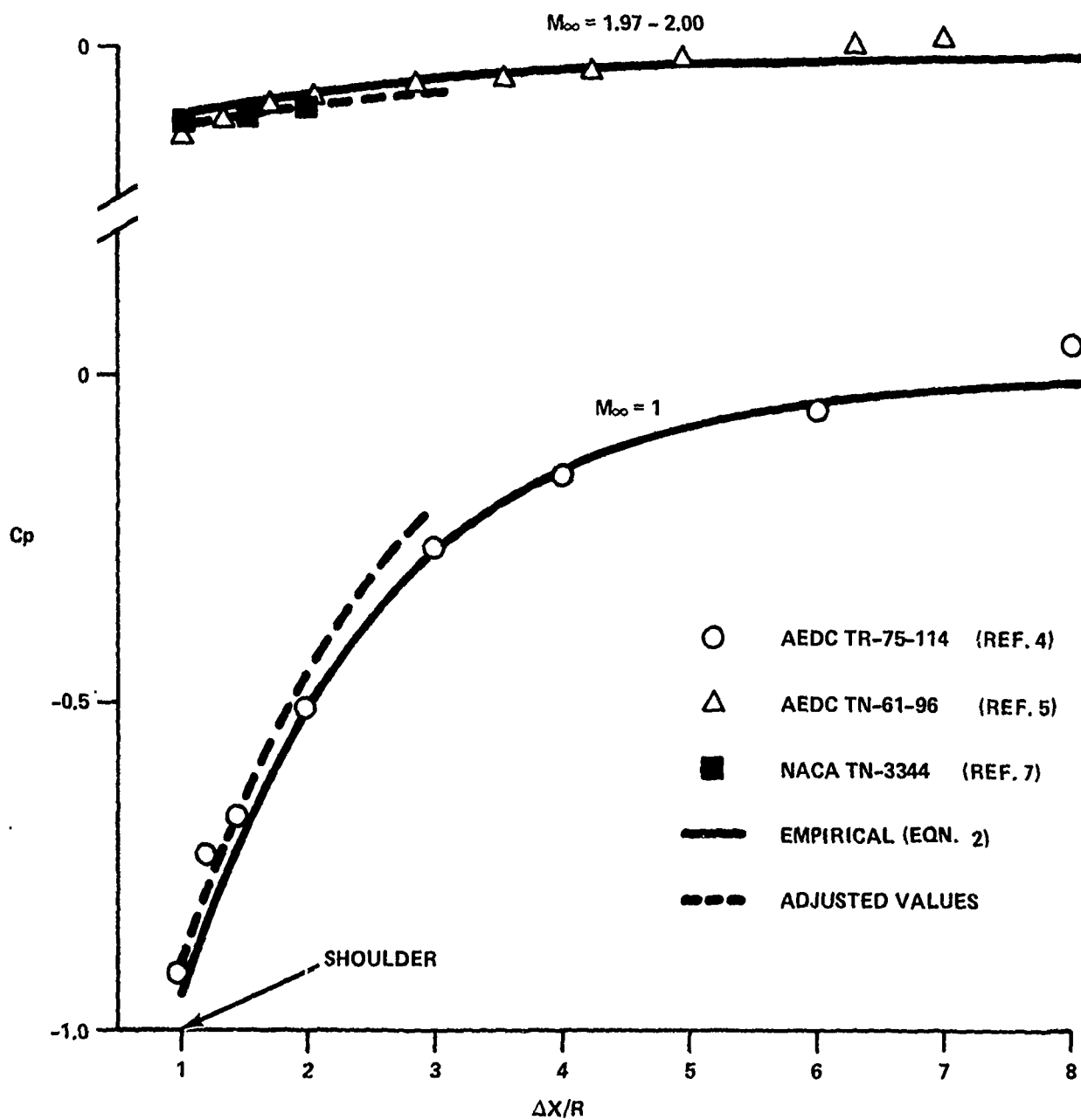


FIGURE 3. LOCAL SURFACE PRESSURE COEFFICIENTS ON A HEMISPHERE-CYLINDER DOWNSTREAM OF THE SHOULDER.

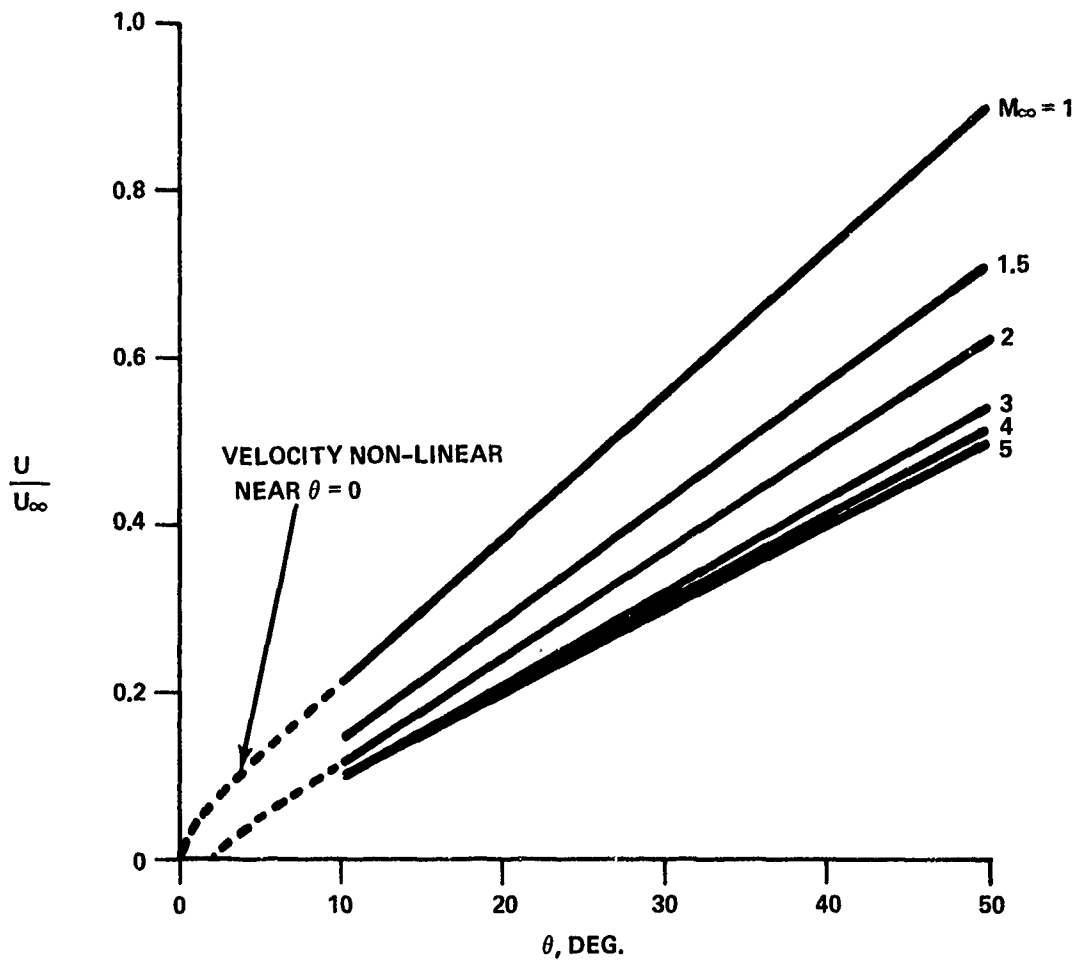
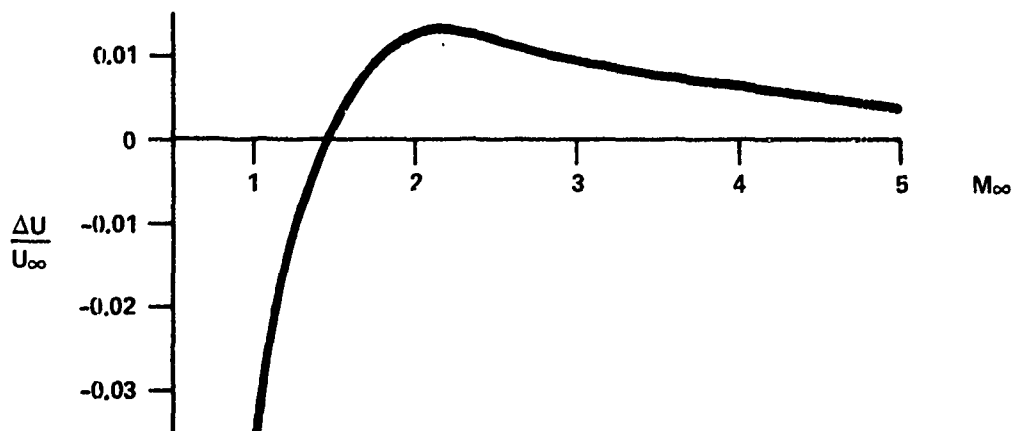
FIGURE 4a. VELOCITY DISTRIBUTION ON A HEMISPHERE FROM ANDREWS' EQN. FOR C_p 

FIGURE 4b. CORRECTIONS TO VELOCITY DISTRIBUTION COMPUTED FROM ANDREW'S EQN.

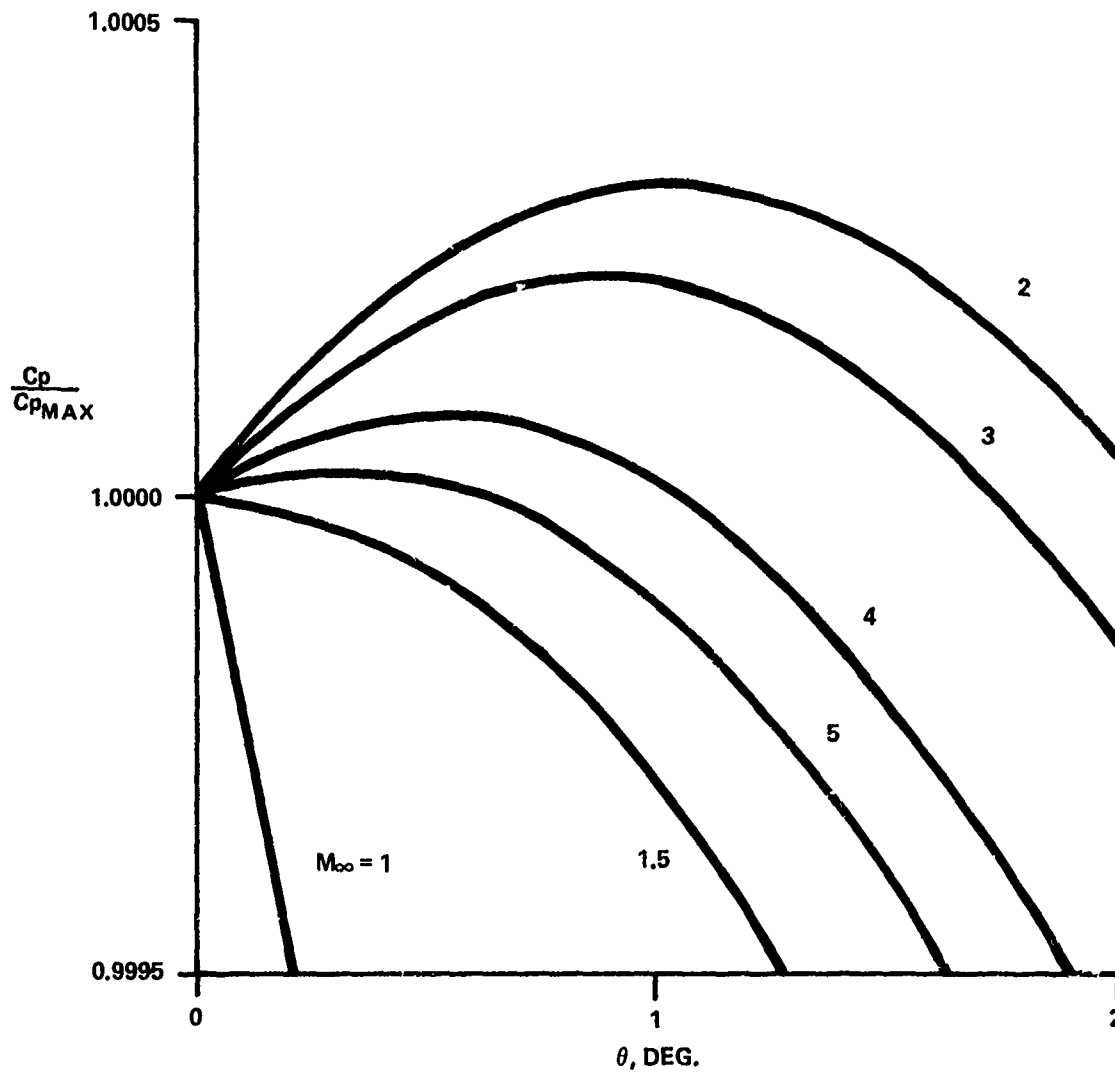


FIGURE 5. PRESSURE COEFFICIENTS NEAR THE STAGNATION POINT ON A HEMISPHERE FROM ANDREWS' EMPIRICAL EQN.

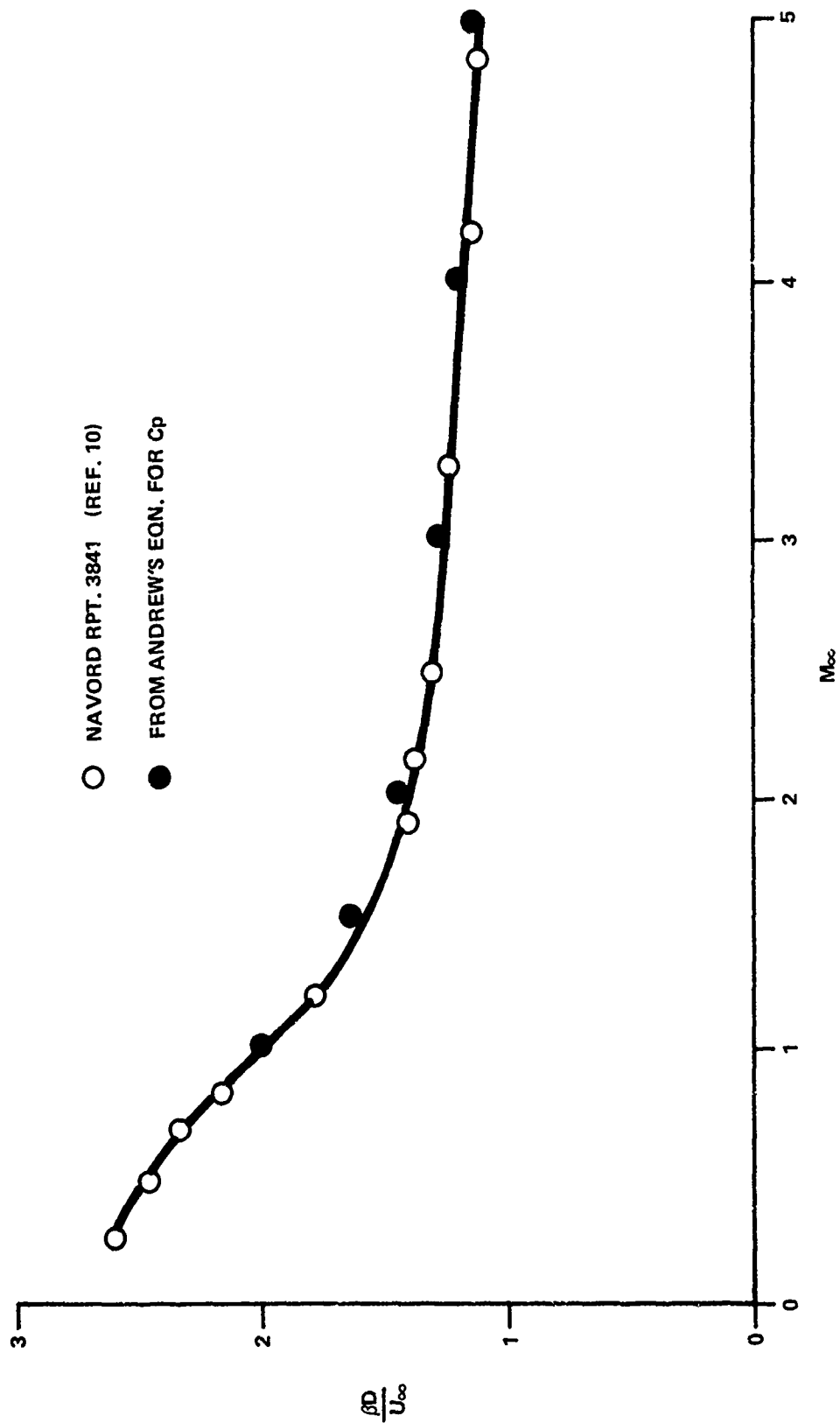
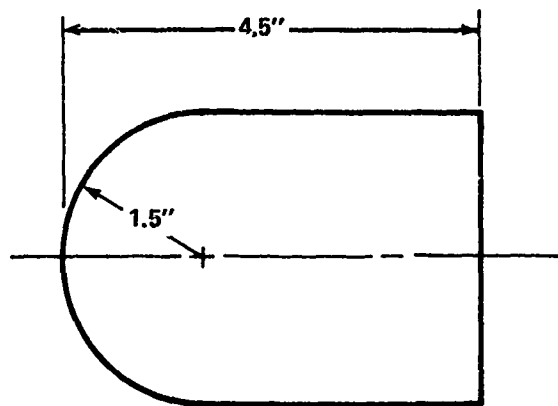


FIGURE 6. NON-DIMENSIONAL VELOCITY GRADIENT AT THE STAGNATION POINT OF A HEMISPHERE.



$t_{\infty} = -12^{\circ}\text{F} = 448^{\circ}\text{R}$
 ALTITUDE $\approx 20,000$ FT
 IDEAL GAS PROPERTIES
 CONSTANT WALL TEMPERATURE

M_{∞}	U_{∞} , FT/SEC	Re_{∞} , D	T_w/T_o
1	1038	1×10^6	0.9
1.5	1556	1.5	0.8
2	2075	2	0.6
3	3113	3	0.5
4	4150	4	0.4
5	5188	5	0.35

FIGURE 7. CONFIGURATION AND CONDITIONS USED IN AEROHEATING CALCULATIONS

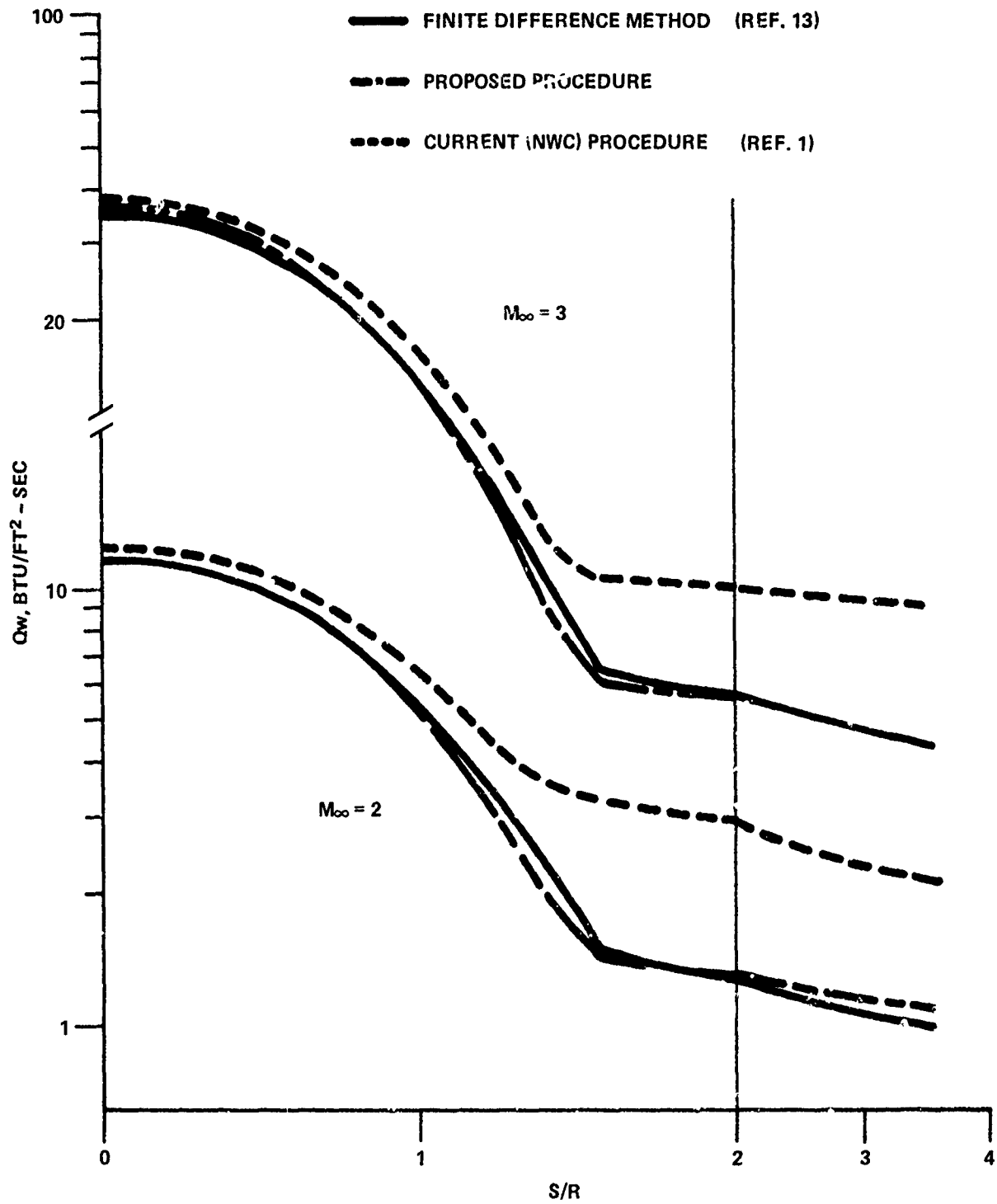


FIGURE 8a. PREDICTED LAMINAR AERODYNAMIC HEATING ON A HEMISPHERE-CYLINDER.

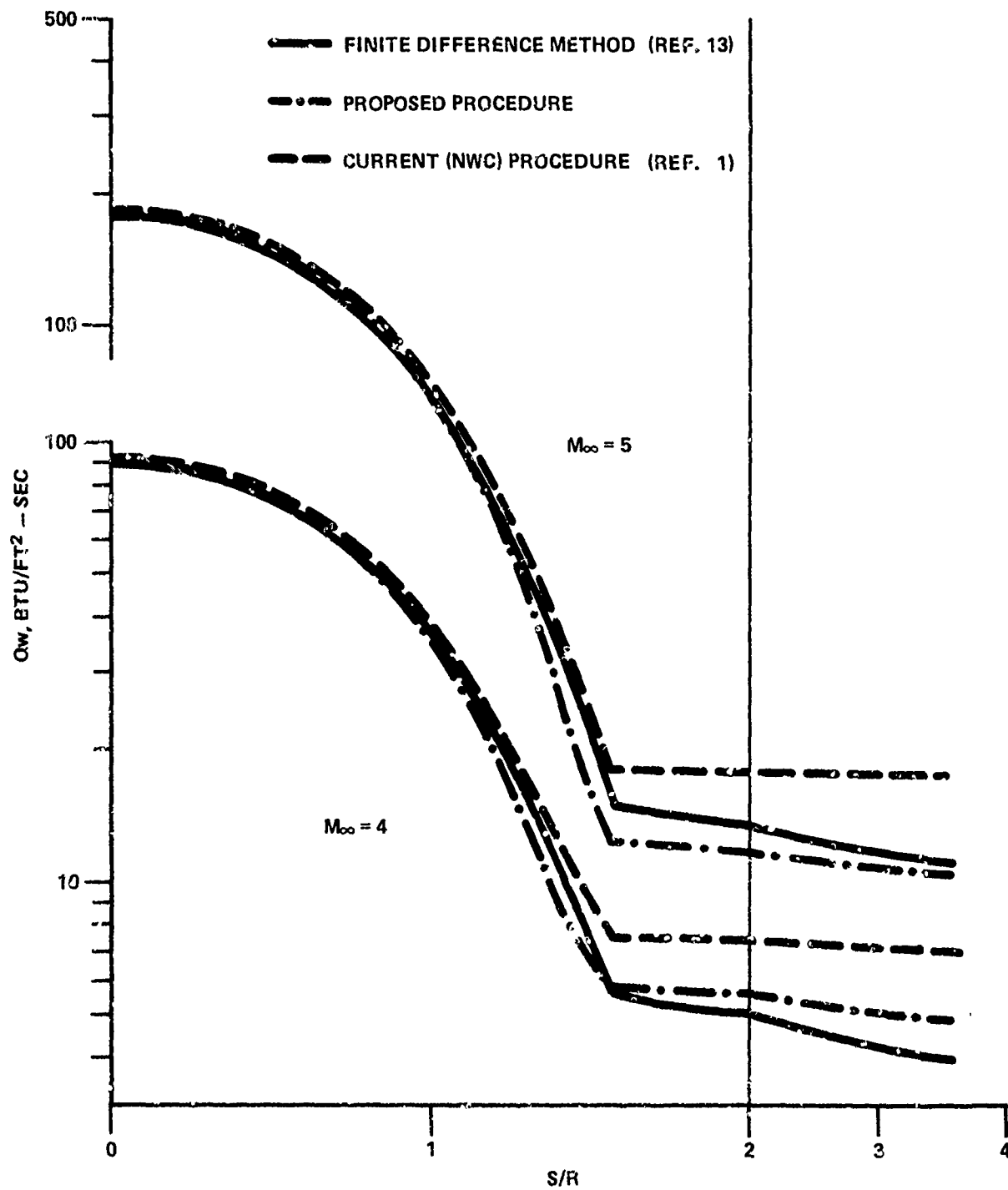


FIGURE 8b. PREDICTED LAMINAR AERODYNAMIC HEATING ON A HEMISPHERE -- CYLINDER

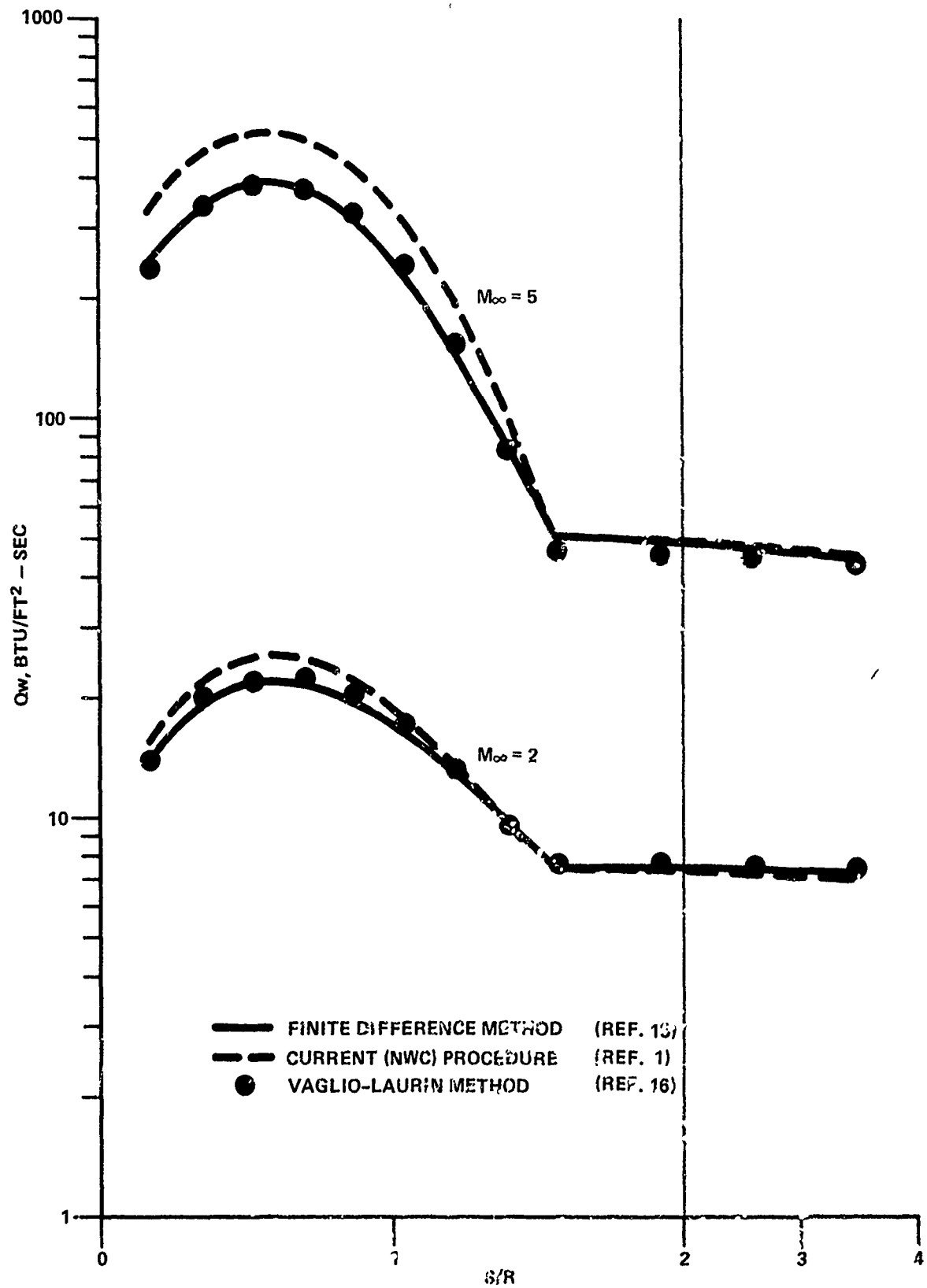


FIGURE 9. PREDICTED TURBULENT AERODYNAMIC HEATING ON A HEMISPHERE - CYLINDER.

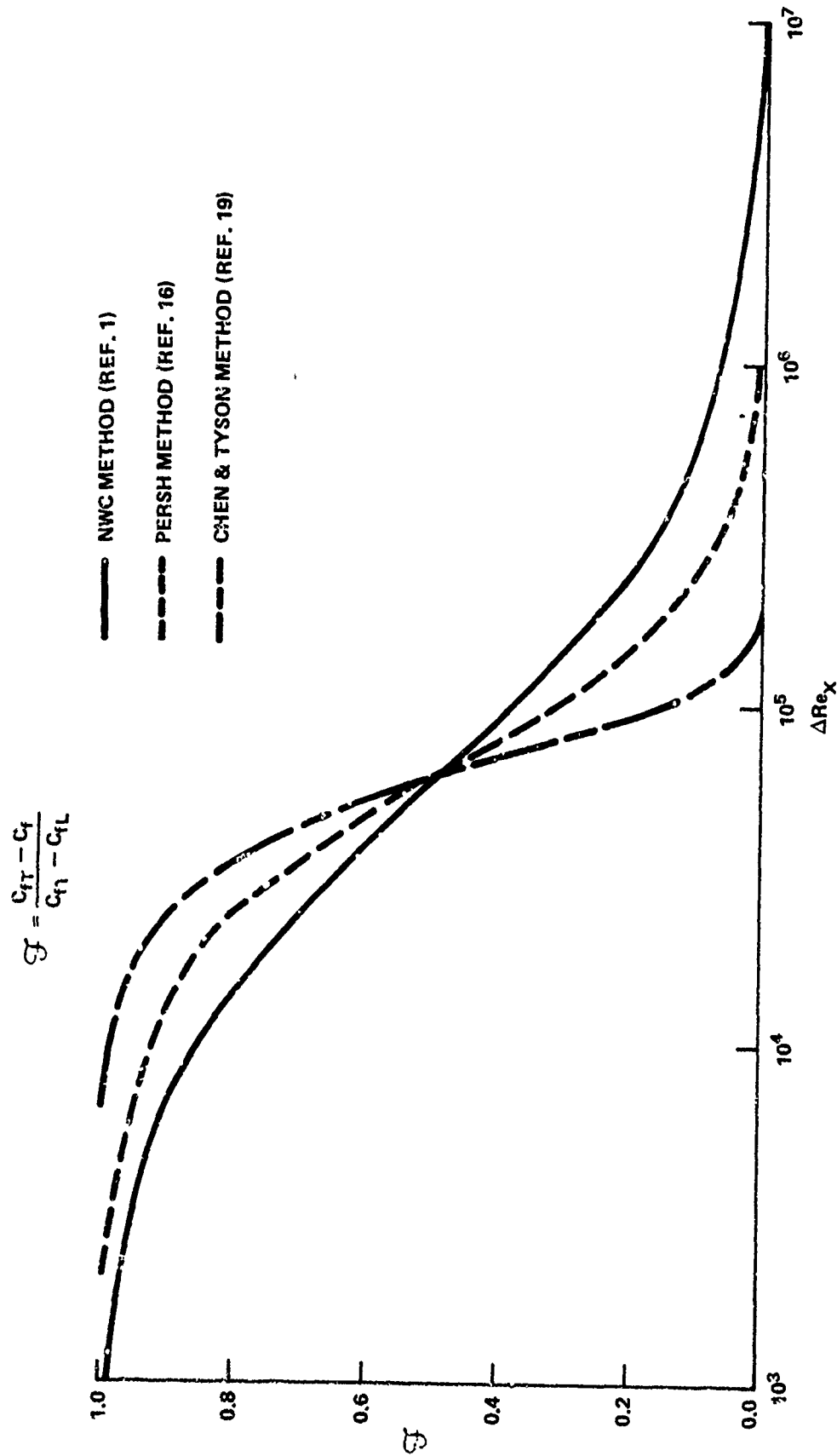


FIGURE 103 TRANSITIONAL SKIN FRICTION FOR INCOMPRESSIBLE FLAT PLATE BOUNDARY LAYER FLOW, $Re_\theta^* = 200$

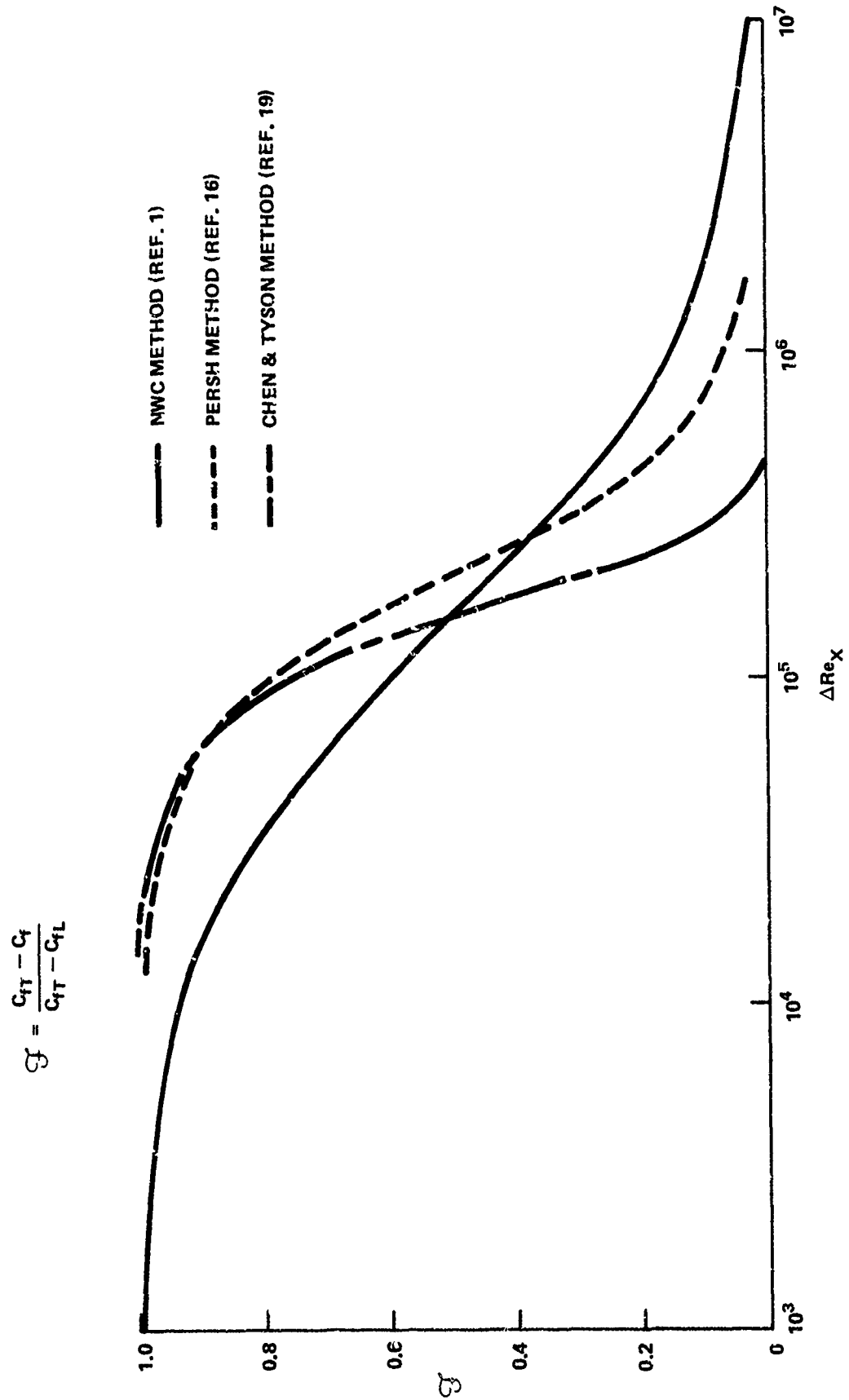


FIGURE 10b TRANSITIONAL SKIN FRICTION FOR INCOMPRESSIBLE FLAT PLATE BOUNDARY LAYER FLOW, $Re_\theta = 400$

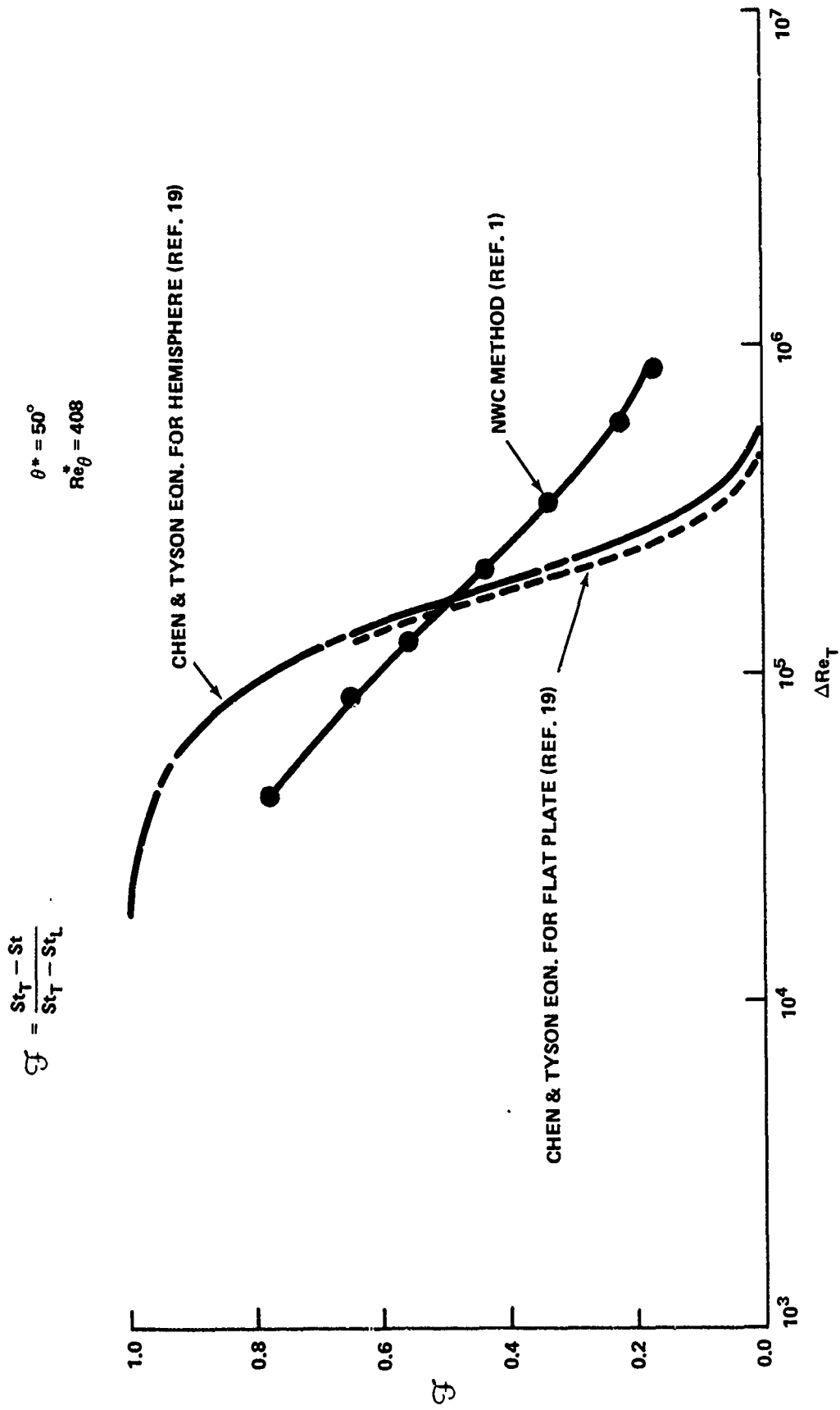


FIGURE 10c TRANSITIONAL HEATING PREDICTIONS ON A HEMISPHERE AT M = 5

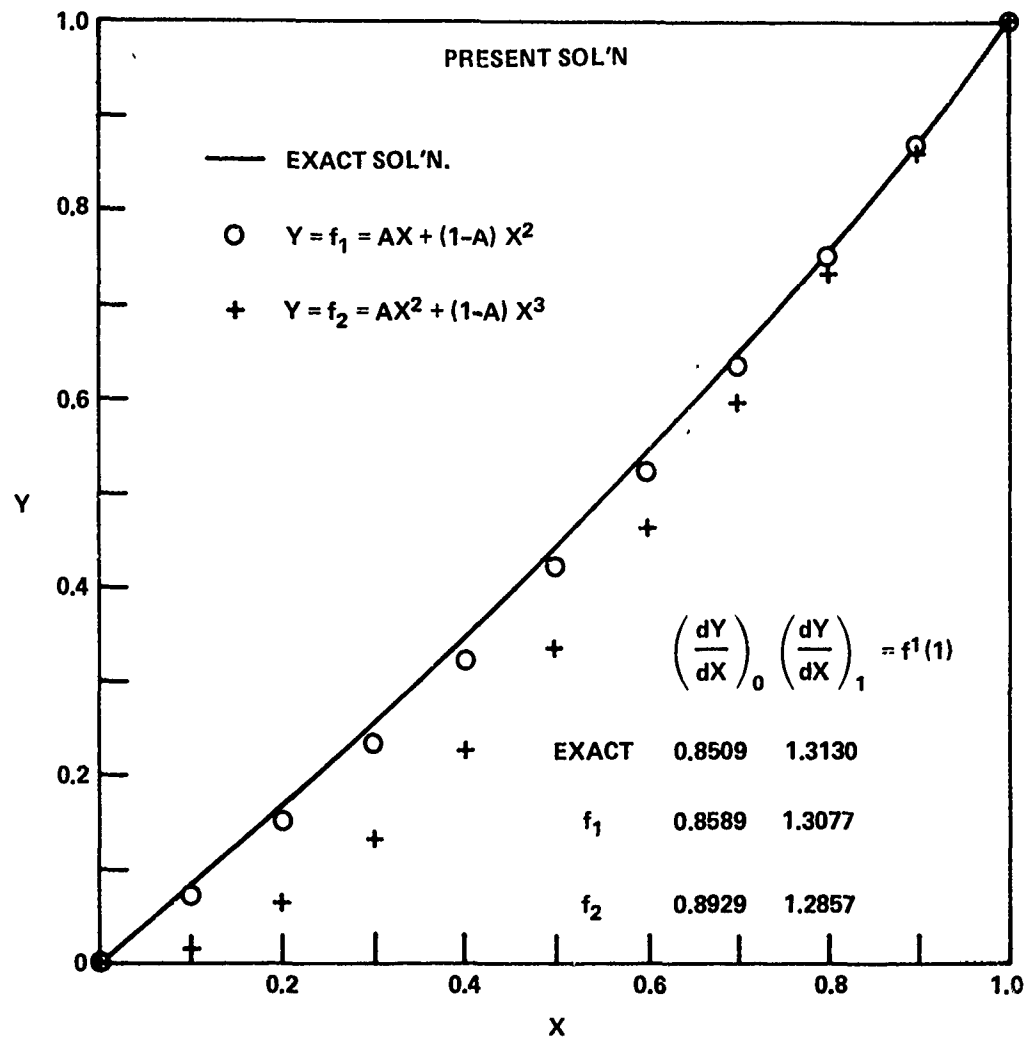


FIGURE 11(a) MODEL PROBLEM: $\frac{d^2Y}{dX^2} = Y$; $Y(0) = 0$, $Y(1) = 1$

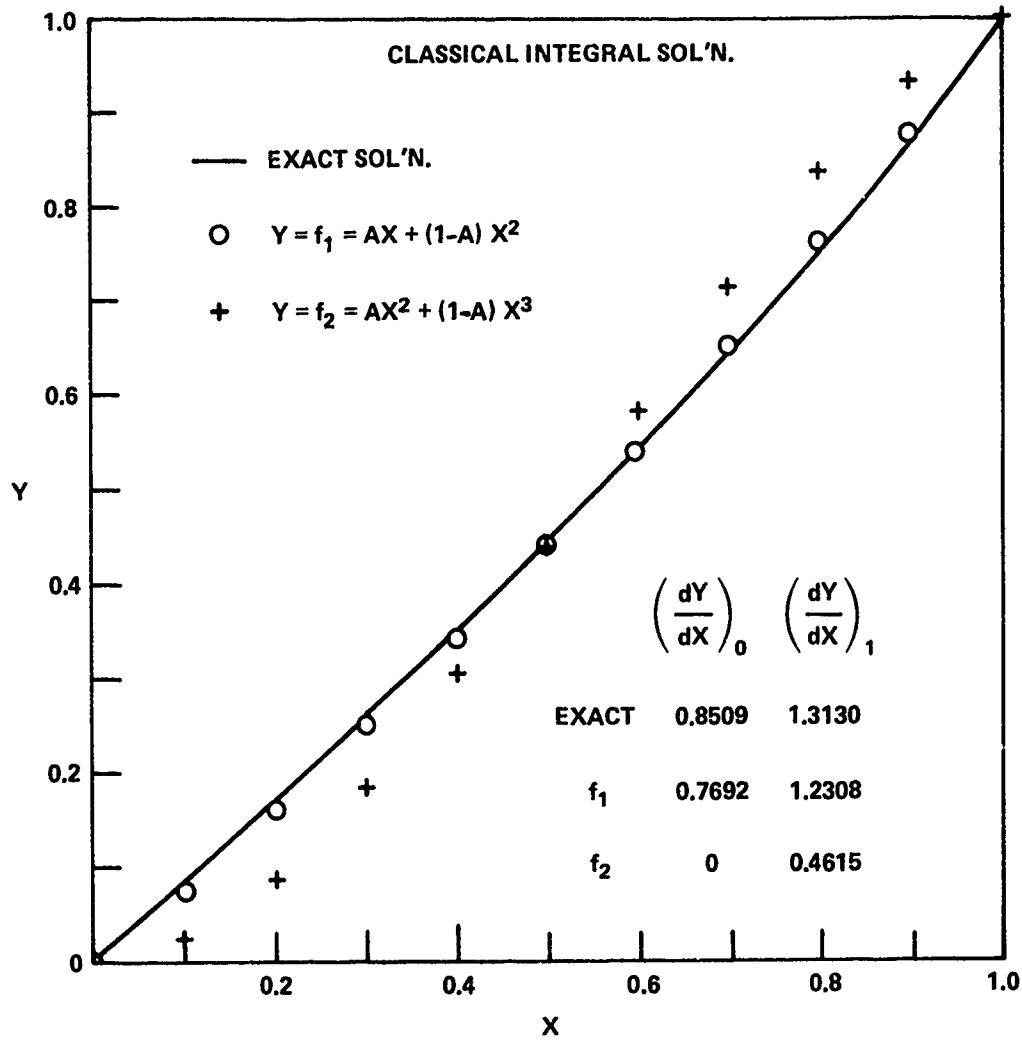


FIGURE 11(b) MODEL PROBLEM, $\frac{d^2Y}{dX^2} = Y$; $Y(0) = 0$, $Y(1) = 1$

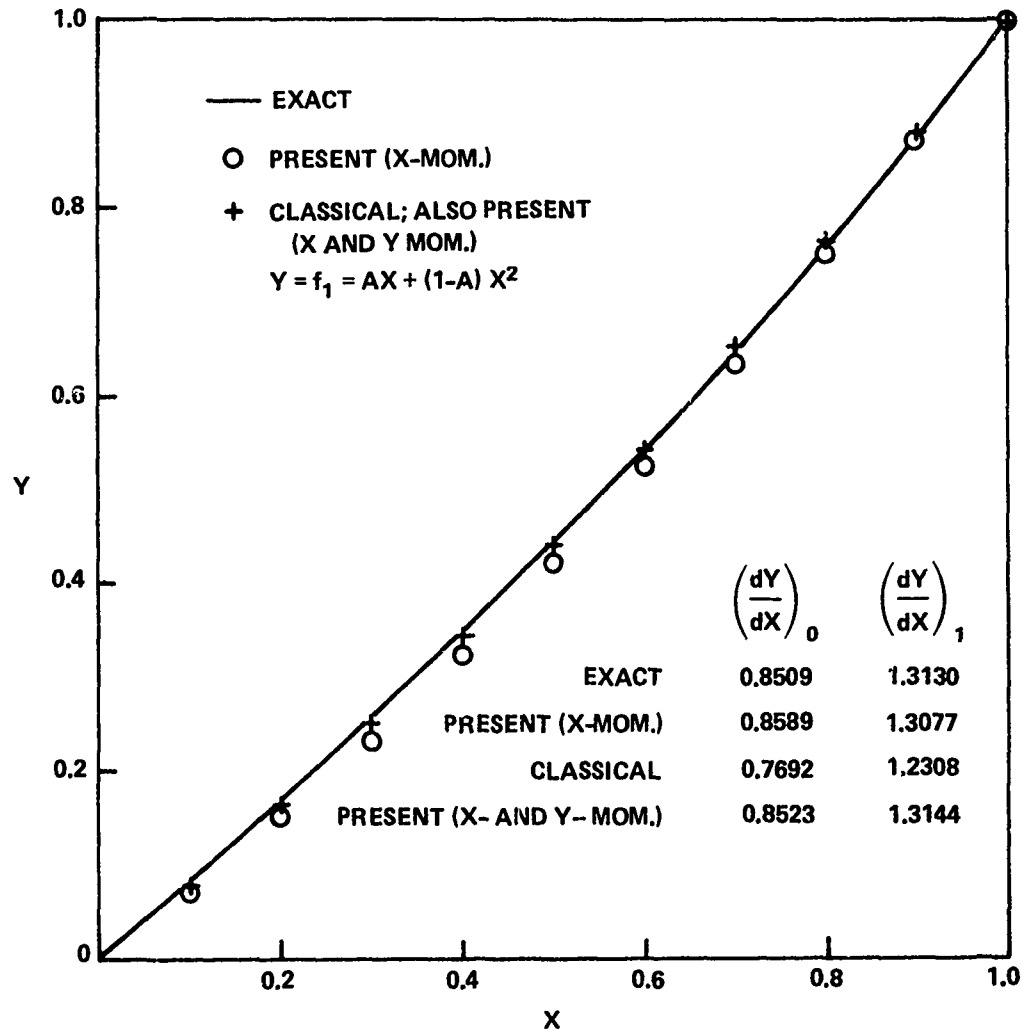


FIGURE 11(c) MODEL PROBLEM, $\frac{d^2Y}{dX^2} = Y$; $Y(0) = 0$, $Y(1) = 1$.

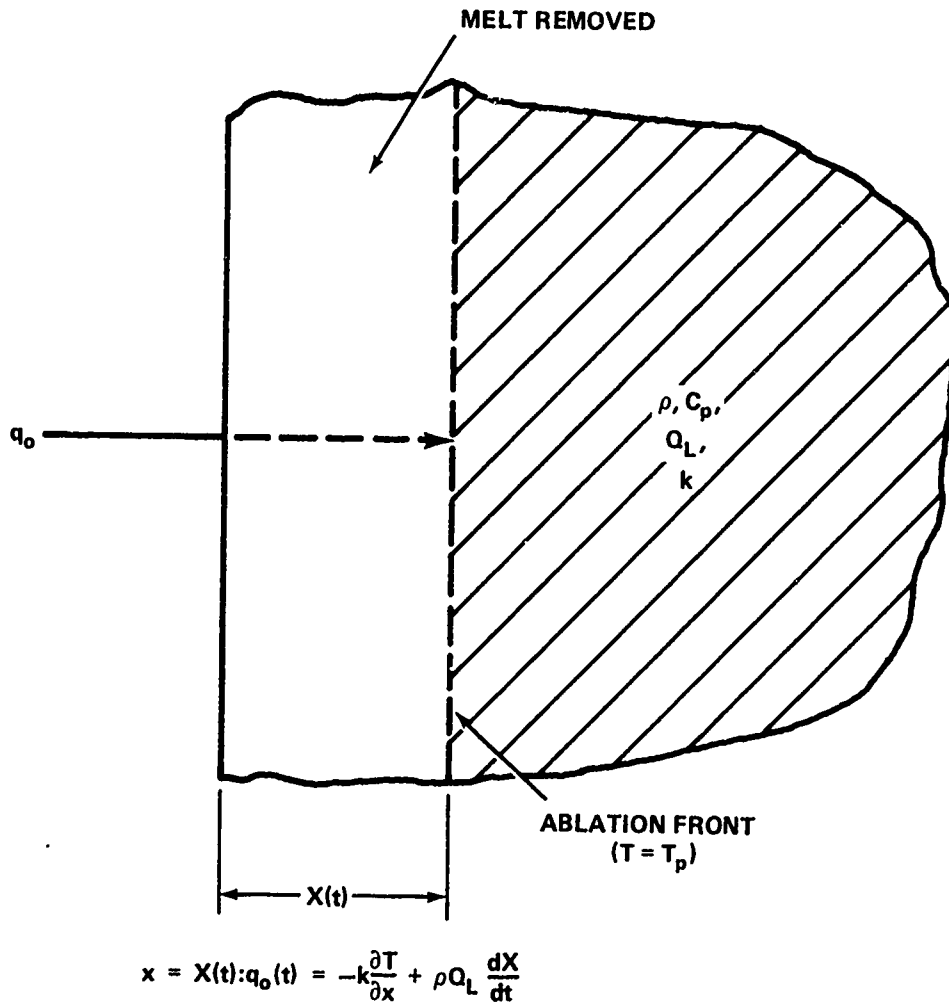
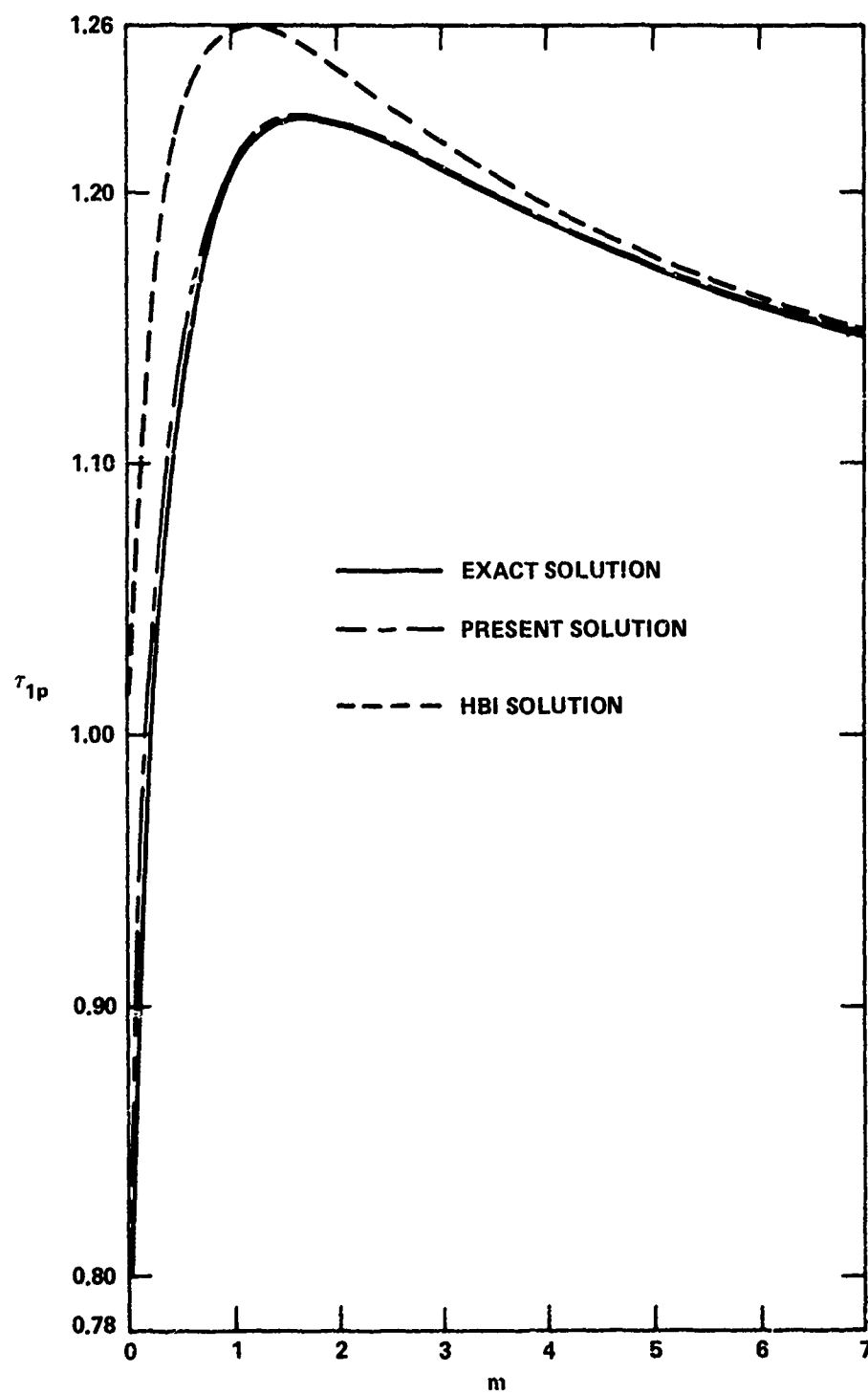
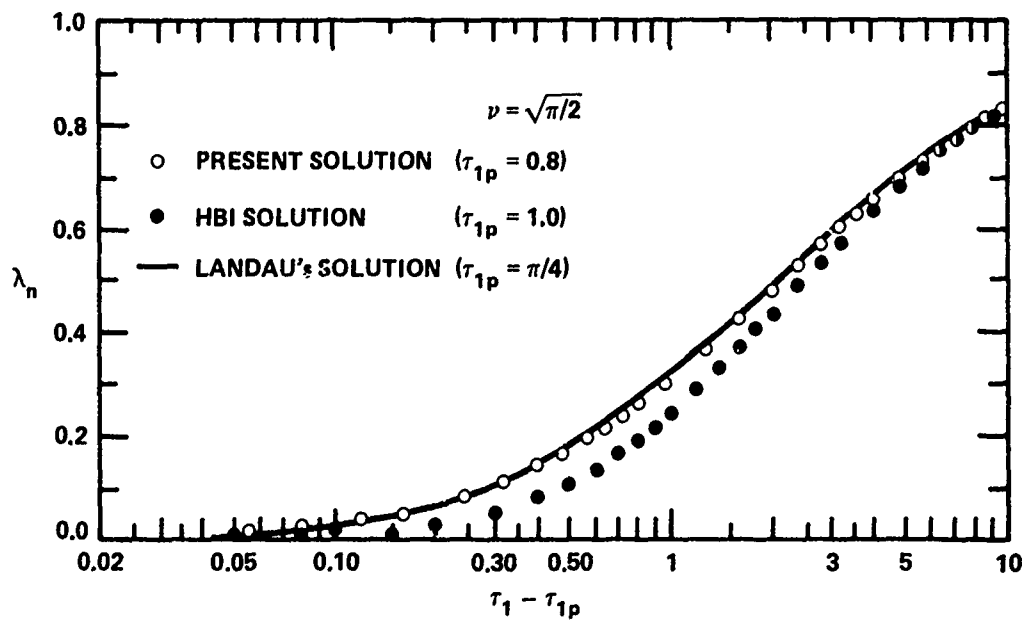


FIGURE 12 ABLATION MODEL

FIGURE 13 PREABLATION TIME FOR $q_0 = At^m (U)$

FIGURE 14 ABLATION THICKNESS: $q_0 = \text{CONST. (U)}$

DISTRIBUTION

Commander
Naval Sea Systems Command
Attn: SEA-05121 (Chief Technical Analyst)
SEA-033
SEA-031
SEA-09G32
Department of the Navy
Washington, DC 20362

2

Commander
Naval Air Systems Command
Attn: AIR-03B
AIR-03C
AIR-320
AIR-320C (William C. Volz)
AIR-310 (Dr. H. J. Mueller)
AIR-50174
Department of the Navy
Washington, DC 20361

2

Office of Naval Research
Attn: ONR-430B (Morton Cooper)
800 N. Quincy Street
Arlington, VA 22203

2

Commander
David W. Taylor Naval Ship Research and
Development Center
Attn: 5641 (Central Library Branch)
5643 (Aerodynamics Laboratory)
Bethesda, MD 20034

Commander
Naval Weapons Center
Attn: 3161 (Bertha Ryan, W. R. Compton,
C. F. Markarian, Ray Van Aken)
533 (Technical Library)
406
4063 (R. E. Meeker)
China Lake, CA 93555

Director
Naval Research Laboratory
Attn: Library
6503
Washington, DC 20390

DISTRIBUTION (Cont.)

NASA

Langley Station

Attn: MS/185 (Technical Library)

Aero & Space Mech Div.

Dennis Bushwell

Ivan Beckwith

R. Trimpi

MS/164 (J. B. Anders)

Hampton, VA 23665

NASA

Lewis Research Center

Attn: 60-3 (Library)

Chief, Wind Tunnel and Flight Division

21000 Brookpart Road

Cleveland, OH 44135

NASA

George C. Marshall Space Flight Center

Attn: R-AERO-AU (T. Reed)

ED31 (W. K. Dahm)

Huntsville, AL 35812

NASA

Attn: RR (Dr. H. H. Kurzweg)

600 Independence Avenue S.W.

Washington, DC 20546

NASA

P. O. Box 33

College Park, MD 20740

Technical Library

Director Defense Research and

Engineering (DDR&E)

Attn: Stop 103

Room 3E-1063, The Pentagon

Washington, DC 20301

Defense Documentation Center

Cameron Station

Alexandria, VA 22314

12

Commander

Naval Missile Center

Attn: Technical Library

Point Mugu, CA 93041

DISTRIBUTION (Cont.)

Commanding Officer
USA Aberdeen Research and Development Center
Attn: STEAP-TL (Technical Library Division)
AMXKD-XSE
Aberdeen Proving Ground, MD 21005

Director
Strategic Systems Project Office
Attn: NSP-2722
Department of the Navy
Washington, DC 20390

2

Director of Intelligence
Attn: AFOIN-3B
Headquarters, USAF (AFNINDE)
Washington, DC 20330

Commander
Space and Missile Systems Organization
Attn: SMTM (LT C. Lee)
Air Force Unit Post Office
Los Angeles Air Force Station, CA 90045

Headquarters
Arnold Engineering Development Center
Attn: Library/Documents (Joe Ashley, Jr.)
R. W. Henzel, TD
DYR (CAPT C. Tirres)
Library/Documents
Arnold Air Force Station, TN 37389

von Karman Gas Dynamics Facility
ARO, Inc.
Attn: Dr. J. D. Whitfield, Chief
Arnold Air Force Station, TN 37389

Commanding Officer
Harry Diamond Laboratories
Attn: Library
Adelphi, MD 20783

Commanding General
U.S. Army Missile Command
Attn: AMSMI-RR
Chief, Document Section
AMSMI-RDX (P. A. Deep)
AMSMI-RDK (T. R. Street)
Redstone Arsenal, AL 35809

2

DISTRIBUTION (Cont.)

Department of the Army
Office of the Chief of Research and Development
ABMDA, The Pentagon
Washington, DC 20350

Commanding Officer
Picatinny Arsenal
Attn: SMUPA-VC-3 (A. A. Loeb)
Dover, NJ 07801

Commander (ADL)
Naval Air Development Center
Warminster, PA 18974

Air Force Weapons Laboratory
Technical Library (SUL)
Kirtland Air Force Base
Albuquerque, NM 87117

U.S. Army Ballistic Missile Defense Agency
Attn: Dr. Sidney Alexander
1300 Wilson Boulevard
Arlington, VA 22209

Applied Physics Laboratory
Attn: Document Library
Dr. F. Hill
Dr. L. L. Cronvich
J. D. Randall
Johns Hopkins University
Johns Hopkins Road
Laurel, MD 20810

2

Director, Defense Nuclear Agency
Attn: STSP (SPAS)
Headquarters DASA
Washington, DC 20305

Commanding Officer
Naval Intelligence Support Center
4301 Suitland Road
Washington, DC 20390

Department of Aeronautics
Attn: COL E. H. Daley, Prof. & Head
DFAN
USAF Academy, CO 80840

DISTRIBUTION (Cont.)

Chief of Naval Research
Attn: ONR 100
Arlington, VA 22217

Air Force Armament Test Laboratory
Attn: C. B. Butler
Eglin Air Force Base, FL 32542

Headquarters, Edgewood Arsenal
Attn: A. Flateau
Edgewood Arsenal, MD 21010

Fluid Mechanics Research Laboratory
Wright-Patterson Air Force Base
Attn: E. G. Johnson, Director
Dayton, OH 45433

5

Commander
U.S. Army
Natick Laboratories
Attn: G. Barnard
STSNL-UBS
Natick, MA 01760

NASA Ames Research Center
Attn: Dr. M. Horstman
Moffett Field, CA 94035

Fluid Dynamics Laboratory
Wright-Patterson Air Force Base
Attn: Dr. D. J. Harney
Dayton, OH 45433

Energetics Laboratory
Wright-Patterson Air Force Base
Attn: Dr. A. W. Fiore
Dayton, OH 45433

Headquarters
Naval Material Command
Attn: LCDR R. D. Matulka
Department of the Navy
Washington, DC 20362

Naval Postgraduate School
Attn: Prof. D. J. Collins
Department of Aeronautics
Monterey, CA 93940

DISTRIBUTION (Cont.)

Aerospace Engineering Program
University of Alabama
Attn: Prof. W. K. Roy, Chm.
P.O. Box 6307
Tuscaloosa, AL 35486

AME Department
University of Arizona
Attn: Dr. L. B. Scott
Tucson, AZ 85721

Polytechnic Institute of Brooklyn
Attn: Dr. J. Polczynski
Graduate Center Library
Route 110, Farmingdale
Long Island, NY 11735

Polytechnic Institute of Brooklyn
Attn: Reference Department
Spicer Library
333 Jay Street
Brooklyn, NY 11201

Brown University
Division of Engineering
Attn: Dr. M. Sibulkin
Library
Providence, RI 02912

California Institute of Technology
Attn: Graduate Aeronautical Laboratories
Aero. Librarian
Karman Lab-301 (Dr. H. Liepmann)
Firestone Flight Sciences Lab.
(Prof. L. Lees)
Guggenheim Lab. (Prof. D. Coles, 321)
Dr. A. Roshko
Pasadena, CA 91109

University of California
Attn: Dr. M. Holt
Dept. of Mechanical Engineering
Berkeley, CA 94720

DISTRIBUTION (Cont.)

GASDYNAMICS

University of California
Attn: A. K. Oppenheim
Richmond Field Station
1301 South 46th Street
Richmond, CA 94804

Department of Aerospace Engineering
University of Southern California
Attn: Dr. John Laufer
University Park
Los Angeles, CA 90007

University of California - San Diego
Attn: Dr. P. A. Libby
Dr. H. K. Cheng
Department of Aerospace and Mechanical
Engineering Sciences
LaJolla, CA 92037

Case Western Reserve University
Attn: Dr. Eli Reshotko, Head
Division of Fluid, Thermal and
Aerospace Engineering
Cleveland, OH 44106

The Catholic University of America
Attn: Dr. C. C. Chang
Dr. Paul K. Chang,
Mechanical Engineering Dept.
Dr. M. J. Casarella,
Mechanical Engineering Dept.
Washington, DC 20017

University of Cincinnati
Attn: Department of Aerospace Engineering
Dr. Arnold Polak
Cincinnati, OH 45221

Department of Aerospace Engineering Sciences
University of Colorado
Boulder, CO 80202

DISTRIBUTION (Cont.)

Cornell University
Attn: Dr. S. F. Shen
Prof. F. K. Moore, Head
Thermal Engineering
Dept., 208 Upson Hall
Graduate School of Aero. Engineering
Ithaca, NY 14850

University of Delaware
Attn: Dr. James E. Danberg
Mechanical and Aeronautical Engineering Dept.
Newark, DE 19711

Georgia Institute of Technology
Attn: Dr. Arnold L. Ducoffe
225 North Avenue, N.W.
Atlanta, GA 30332

Technical Reports Collection
Gordon McKay Library
Harvard University
Division of Engineering and Applied Physics
Pierce Hall
Oxford Street
Cambridge, MA 02138

Illinois Institute of Technology
Attn: Dr. M. V. Morkovin
Prof. A. A. Fejer, M.A.E. Dept.
3300 South Federal
Chicago, IL 60616

University of Illinois
Aeronautical and Astronautical Engineering
Department
101 Transportation Bldg.
Urbana, IL 61801

Iowa State University
Aerospace Engineering Dept.
Ames, Iowa 50010

The Johns Hopkins University
Attn: Professor S. Corrsin
Baltimore, MD 21218

DISTRIBUTION (Cont.)

University of Kentucky
Attn: C. F. Knapp
Wenner-Gren Aero. Lab.
Lexington, KY 40506

Department of Aero. Engineering, ME 106
Louisiana State University
Attn: Dr. P. H. Miller
Baton Rouge, LA 70803

University of Maryland
Attn: Prof. A. Wiley Sherwood,
Department of Aerospace Engineering
Prof. Charles A. Shreeve
Department of Mechanical Engineering
Dr. S. I. Pai, Institute for Fluid
Dynamics and Applied Mathematics
Dr. Redfield W. Allen, Department
of Mechanical Engineering
Dr. W. L. Melnik, Department of
Aerospace Engineering
Dr. John D. Anderson, Jr.
Department of Aerospace Engineering
College Park, MD 20740

Michigan State University
Attn: Library, Documents Department
East Lansing, MI 48823

Massachusetts Institute of Technology
Attn: Mr. J. R. Martuccelli, Rm. 33-211
Prof. M. Finston
Prof. J. Baron, Dept. of Aero. and
Astro., Rm. 37-461
Prof. A. H. Shapiro, Head, Mech.
Engr. Dept.
Aero. Engineering Library
Prof. Ronald F. Probestein
Dr. E. E. Covert
Aerophysics Laboratory
Cambridge, MA 02139

University of Michigan
Attn: Dr. M. Sichel, Dept. of Aero. Engr.
Engineering Library
Aerospace Engineering Lib.
Mr. C. Cousineau, Engin-Trans Lib.
Dr. C. M. Vest, Dept. of Mech. Engr.
Ann Arbor, MI 48104

DISTRIBUTION (Cont.)

Serials and Documents Section
General Library
University of Michigan
Ann Arbor, MI 48104

Mississippi State University
Attn: Mr. Charles B. Cliett
Department of Aerophysics and
Aerospace Engineering
P.O. Drawer A
State College, MS 39762

U.S. Naval Academy
Engineering Department, Aerospace Division
Annapolis, MD 21402

U.S. Naval Postgraduate School
Library, Code 2124
Attn: Technical Reports Section
Monterey, CA 93940

New York University
Attn: Dr. Antonio Ferri, Director of
Guggenheim Aerospace Laboratories
Prof. V. Zakkay
Engineering and Science Library
University Heights
New York, NY 10453

North Carolina State College
Attn: Dr. F. R. DeJarnette, Dept. Mech.
and Aero. Engineering
Dr. H. A. Hassan, Dept. of Mech.
and Aero. Engineering
Raleigh, NC 27607

North Carolina State University
Attn: D. H. Hill Library
P.O. Box 5007
Raleigh, NC 27607

University of North Carolina
Attn: Department of Aero. Engineering
Library, Documents Section
APROTC Det 590
Chapel Hill, NC 27514

DISTRIBUTION (Cont.)

Northwestern University
Technological Institute
Attn: Department of Mechanical Engineering
Library
Evanston, IL 60201

Notre Dame University
Attn: Dr. J. D. Nicolaides, Dept. of
Aero. Engineering
College of Engineering Library
South Bend, IN 46556

Department of Aero-Astro Engineering
Ohio State University
Attn: Engineering Library
Prof. J. D. Lee
Prof. G. L. Von Eschen
2036 Neil Avenue
Columbus, OH 43210

Ohio State University Libraries
Documents Division
1858 Neil Avenue
Columbus, OH 43210

The Pennsylvania State University
Attn: Dept. of Aero Engr., Hammond Bldg.
Library, Documents Section
University Park, PA 18602

Bevier Engineering Library
126 Benedum Hall
University of Pittsburgh
Pittsburgh, PA 15261

Princeton University
Attn: Prof. S. Bogdonoff
Dr. I. E. Vas
Aerospace & Mechanical Science Dept.
D-214 Engrg. Quadrangle
Princeton, NJ 08540

Purdue University
School of Aeronautical and Engineering
Sciences
Attn: Library
Dr. P. S. Lykoudis, Dept. of Aero.
Engineering
Lafayette, IN 47907

DISTRIBUTION (Cont.)

Rensselaer Polytechnic Institute
Attn: Dept. of Aeronautical Engineering
and Astronautics
Troy, NY 12181

Rutgers - The State University
Attn: Dr. R. H. Page
Dr. C. F. Chen
Department of Mechanical Industrial and
Aerospace Engineering
New Brunswick, NJ 08903

Stanford University
Attn: Librarian, Dept. of Aeronautics and
Astronautics
Stanford, CA 94305

Stevens Institute of Technology
Attn: Mechanical Engineering Department
Library
Hoboken, NJ 07030

The University of Texas at Austin
Attn: Engr S.B.114B, Dr. Friedrich
Applied Research Laboratories
P.O. Box 8029
Austin, TX 78712

University of Toledo
Attn: Dept. of Aero. Engineering
Dept. of Mech. Engineering
2801 W. Bancroft
Toledo, OH 43606

University of Virginia
School of Engineering and Applied Science
Attn: Dr. I. D. Jacobson
Dr. G. Matthews
Dr. R. N. Zapata
Charlottesville, VA 22901

University of Washington
Attn: Engineering Library
Dept. of Aeronautics and Astronautics
Prof. R. E. Street, Dept. of Aero.
and Astro.
Prof. A. Hertzberg, Aero. and Astro.,
Guggeheim Hall
Seattle, WA 98105

DISTRIBUTION (Cont.)

West Virginia University
Attn: Library
Morgantown, WV 26506

Federal Reports Center
University of Wisconsin
Attn: S. Reilly
Mechanical Engineering Building
Madison, WI 53706

Los Alamos Scientific Laboratory
Attn: Report Library
P.O. Box 1663
Los Alamos, NM 87544

University of Maryland
Attn: Dr. R. C. Roberts,
Mathematics Department
Baltimore County (UMBC)
5401 Wilkens Avenue
Baltimore, MD 21228

Institute for Defense Analyses
Attn: Classified Library
400 Army-Navy Drive
Arlington, VA 22202

Kaman Sciences Corporation
Attn: Library
P.O. Box 7463
Colorado Springs, CO 80933

Kaman Science Corporation
Attn: Dr. J. R. Ruetenik
Avidyne Division
83 Second Avenue
Burlington, MA 01803

Rockwell International
B-1 Division
Technical Information Center (BA08)
International Airport
Los Angeles, CA 90009

Rockwell International Corporation
Technical Information Center
4300 E. Fifth Avenue
Columbus, OH 43216

DISTRIBUTION (Cont.)

M.I.T. Lincoln Laboratory
Attn: Library A-082
P.O. Box 73
Lexington, MA 02173

The RAND Corporation
Attn: Library - D
1700 Main Street
Santa Monica, CA 90406

Aerojet Electrosystems Co.
Attn: Engineering Library
1100 W. Hollyvale Avenue
Azusa, CA 91702

The Boeing Company
Attn: 87-67
P.O. Box 3999
Seattle, WA 98124

United Aircraft
Research Laboratories
Attn: Dr. William M. Foley
East Hartford, CT 06108

United Aircraft Corporation
Attn: Library
400 Main Street
East Hartford, CT 06108

Hughes Aircraft Company
Attn: Company Tech. Doc. Center
6/E11, B. W. Campbell
Centinela at Teale
Culver City, CA 90230

Lockheed Missiles and Space Company, Inc.
Attn: Mr. G. M. Laden, Dept. 81-25,
Bldg. 154
Mr. Murl Culp
P.O. Box 504
Sunnyvale, CA 94086

Lockheed Missiles and Space Company
Attn: Technical Information Center
3251 Hanover Street
Palo Alto, CA 94304

DISTRIBUTION (Cont.)

Lockheed-California Company
Attn: Central Library, Dept. 84-40,
Bldg. 170
PLT. B-1
Burbank, CA 91503

Vice President and Chief Scientist
Dept. 03-10
Lockheed Aircraft Corporation
P.O. Box 551
Burbank, CA 91503

Martin Marietta Corporation
Martin Marietta Labs
Attn: Science-Technology Library
1450 S. Rolling Road
Baltimore, MD 21227

Martin Marietta Corporation
Orlando Division
P.O. Box 5837
Orlando, FL 32855

General Dynamics
Attn: Research Library 2246
George Kaler, Mail Zone 2880
P.O. Box 748
Fort Worth, TX 76101

Calspan Corporation
Attn: Library
4455 Genesee Street
Buffalo, NY 14221

Air University Library
(SE) 63-578
Maxwell Air Force Base, AL 36112

McDonnell Company
Attn: R. D. Detrich, Dept. 209,
Bldg. 33
P.O. Box 516
St. Louis, MO 63166

DISTRIBUTION (Cont.)

McDonnell-Douglas Aircraft Corporation
Missile and Space Systems Division
Attn: A2-260 Library
Dr. J. S. Murphy, A-830
Mr. W. H. Branch, Director
300 Ocean Park Boulevard
Santa Monica, CA 90405

Fairchild Industries, Inc.
Fairchild Republic Co.
Attn: Engineering Library
Conklin Street
Farmingdale, NY 11735

General Applied Science Laboratories, Inc.
Attn: Dr. F. Lane
Merrick and Stewart Avenues
Westbury, Long Island, NY 11590

General Electric Company
Attn: Dr. H. T. Nagamatsu
Research and Development Lab. (Comb. Bldg.)
Schenectady, NY 12301

The Whitney Library
General Electric Research and Development Center
Attn: M. F. Orr, Manager
The Knolls, K-1
P.O. Box 8
Schenectady, NY 12301

General Electric Company
Missile and Space Division
Attn: MSD Library
Larry Chasen, Mgr.
Dr. J. D. Stewart, Mgr.
Research and Engineering
P.O. Box 8555
Philadelphia, PA 19101

General Electric Company
AEG Technical Information Center, N-32
Cincinnati, OH 45215

DISTRIBUTION (Cont.)

General Electric Company
Missile and Space Division

Attn: Dr. S. M. Scala
Dr. H. Lew
Mr. J. W. Faust
A. Martellucci
W. Daskin
J. D. Cresswell
J. B. Arnaiz
L. A. Marshall
J. Cassanto
R. Hobbs
C. Harris
F. George

P.O. Box 8555
Philadelphia, PA 19101

AVCO-Everett Research Laboratory

Attn: Library
Dr. George Sutton
2385 Revere Beach Parkway
Everett, MA 02149

2

Vought Corporation
P.O. Box 225907
Dallas, TX 75265

Northrop Corp.
Electronic Division
2301 W. 120th Street
Hawthorne, CA 90250

Government Documents
The Foundren Library
Rice Institute
P.O. Box 1892
Houston, TX 77001

DISTRIBUTION (Cont.)

Grumman Aerospace Corporation
Attn: Mr. R. A. Scheuing
 Mr. H. B. Hopkins
 Mr. H. R. Reed
South Oyster Bay Road
Bethpage, Long Island, NY 11714

The Marquardt Company
P.O. Box 2013
Van Nuys, CA 91409

ARDE Associates
Attn: Librarian
P.O. Box 286
580 Winters Avenue
Paramus, NJ 07652

Aerophysics Company
Attn: Mr. G. D. Boehler
3500 Connecticut Avenue, N.W.
Washington, DC 20003

Aeronautical Research Associates
of Princeton
Attn: Dr. C. duP. Donaldson
50 Washington Road
Princeton, NJ 08540

General Research Corporation
Attn: Technical Information Office
5383 Hollister Avenue
P.O. Box 3587
Santa Barbara, CA 93105

Sandia Laboratories
Attn: Mr. K. Goin, Div. 5642
 Mrs. B. R. Allen, 3421
 Mr. W. H. Curry, 5625
 Mr. A. M. Torneby, 3141
 Dr. C. Peterson
Box 5800
Albuquerque, NM 87115

Hercules Incorporated
Attn: Library
Allegany Ballistics Laboratory
P.O. Box 210
Cumberland, MD 21502

DISTRIBUTION (Cont.)

General Electric Company
Attn: Dave Novis, Rm. 4109
P.O. Box 2500
Daytona Beach, FL 32015

TRW Defense & Space Systems Group
Attn: Technical Libr/Doc Acquisitions
Dr. A. B. Witte
One Space Park
Redondo Beach, CA 90278

Stanford Research Institute
Attn: Dr. G. Abrahamson
333 Ravenswood Avenue
Menlo Park, CA 94025

Hughes Aircraft Company
Attn: Technical Library, 600-C222
P.O. Box 3310
Fullerton, CA 92634

Westinghouse Electric Corporation
Astronuclear Laboratory
Attn: Library
P.O. Box 10864
Pittsburgh, PA 15236

University of Tennessee
Space Institute
Attn: Prof. J. M. Wu
Tullahoma, TN 37388

CONVAIR Division of General Dynamics
Library and Information Services
P.O. Box 12009
San Diego, CA 92112

CONVAIR Division of General Dynamics
Attn: Dr. J. Raat, Mail Zone 640-02
P.O. Box 80847
San Diego, CA 92138

AVCO Missiles Systems Division
Attn: E. E. H. Schurmann
J. Otis
201 Lowell Street
Wilmington, MA 01887

NSWC TR 79-21

DISTRIBUTION (Cont.)

Chrysler Corporation
Space Division
Attn: G. T. Boyd, Dept. 2781
E. A. Rawk, Dept. 2920
P.O. Box 29200
New Orleans, LA 70129

General Dynamics
Pomona Division
Attn: Tech. Doc. Center, Mail Zone 6-20
P.O. Box 2507
Pomona, CA 91766

General Electric Company
Attn: W. Danskin
Larry Chasen
Dr. H. Lew
3198 Chesnut Street
Philadelphia, PA 19101

Ford Aerospace & Communication Corporation
Attn: Dr. A. Demetriades
Ford and Jamboree Roads
Newport Beach, CA 92663

Raytheon Company
Attn: D. P. Forsmo
Missile Systems Division
Hartwell Road
Bedford, MA 01730

TRW Systems Group
Attn: M. W. Sweeney, Jr.
Space Park Drive
Houston, TX 77058

Marine Bioscience Laboratory
Attn: Dr. A. C. Charters
513 Sydnor Street
Ridgecrest, CA 93555

University of California - Los Angeles
Attn: Prof. J. D. Cole
Dept. of Mechanics & Structures
Los Angeles, CA 90024

DISTRIBUTION (Cont.)

University of Wyoming
Attn: Head, Dept. Mech. Eng.
University Station
P.O. Box 3295
Laramie, WY 82070

Applied Mechanics Review
Southwest Research Institute
8500 Culebra Road
San Antonio, TX 78228

American Institute of Aeronautics
and Astronautics
Attn: J. Newbauer
1290 Sixth Avenue
New York, NY 10019

Technical Information Service
American Institute of Aeronautics and
Astronautics
Attn: Miss P. Marshall
750 Third Avenue
New York, NY 10017

Faculty of Aeronautical Systems
University of West Florida
Attn: Dr. R. Fledderman
Pensacola, FL 32504

Saber Industries, Inc.
Attn: J. A. Finkel
Library
P.O. Box 60
North Troy, VT 05859

Pratt and Whitney Aircraft
Attn: W. G. Alwang, EB-1M5
East Hartford, CT 06108

Science Applications, Inc.
Attn: Dr. J. D. Trolinger
P.O. Box 861
Tullahoma, TN 37388

The Aerospace Corporation
Attn: J. M. Lyons, Bldg. 82
P.O. Box 92957
Los Angeles, CA 90009

TO AID IN UPDATING THE DISTRIBUTION LIST
FOR NAVAL SURFACE WEAPONS CENTER, WHITE
OAK TECHNICAL REPORTS PLEASE COMPLETE THE
FORM BELOW:

TO ALL HOLDERS OF NSWC/TR 79-21
by T. F. Zien, Code R-44
DO NOT RETURN THIS FORM IF ALL INFORMATION IS CURRENT

A. FACILITY NAME AND ADDRESS (OLD) (Show Zip Code)

NEW ADDRESS (Show Zip Code)

B. ATTENTION LINE ADDRESSES:

C.

☐ REMOVE THIS FACILITY FROM THE DISTRIBUTION LIST FOR TECHNICAL REPORTS ON THIS SUBJECT.

D.

NUMBER OF COPIES DESIRED _____

DEPARTMENT OF THE NAVY
NAVAL SURFACE WEAPONS CENTER
WHITE OAK, SILVER SPRING, MD. 20910

OFFICIAL BUSINESS
PENALTY FOR PRIVATE USE, \$300

POSTAGE AND FEES PAID
DEPARTMENT OF THE NAVY
DOD 316



COMMANDER
NAVAL SURFACE WEAPONS CENTER
WHITE OAK, SILVER SPRING, MARYLAND 20910

ATTENTION: CODE R-44